RESEARCH

Extreme precipitation and temperature indices under future climate change in central Asia based on CORDEX-CORE

Praveen Rai[1] · Freddy Bangelesa[1,3] · Daniel Abel[1] · Katrin Ziegler[1] · Jingshui Huang[2] ·
Timo Schaffhauser[2] · Felix Pollinger[1] · Markus Disse[2] · Heiko Paeth[1]

Abstract

The present study analyzes the projected changes of extreme climate indices over Central Asia using regional climate model (RCM) simulations from the Coordinated Regional Climate Downscaling Experiment (CORDEX) - Coordinated Output for Regional Evaluations (CORE). The extreme indices are based on precipitation and temperature and are inspected for present (1981–2005) and future periods - near- (2031–2055) and far-future (2071–2095) - to assess the long-term climate change under the representative concentration pathway RCP8.5. Projected changes are analyzed for three different model ensembles. These ensembles are based on CORDEX-Central Asia (ENS_CAS, four ensemble members) and CORDEX-East Asia (ENS_EAS, six ensemble members), and a combination of both (ENS, ten ensemble members) for our study area centered over high mountain Asia, called Central East Asia (CEAS). For precipitation indices, an increase of consecutive dry days (CDD) in ENS_EAS and a slight to moderate decrease in northern parts in ENS_CAS during near-future is observed. Consecutive wet days (CWD), very heavy precipitation events (R20mm), maximum one-day precipitation (RX1day), and very wet days (R95p) are projected to increase in most areas. All indices show a further intensification towards the end of the century over large parts of the domain, e.g., +7.8% / +5.6 days for CDD, +96.6% / +0.26 days for R20mm, and +19.7% for RX1day as median of ENS over CEAS. For temperature indices, the ensembles project a strong increase over the high mountain regions and southern parts for consecutive summer days (CSU, +108.5% / +38.3 days), heat wave duration index (HWDI, +1379.1% / +91.37 days), and the percentage of very hot days (TX90p, +391.1% / +34.54 days). Accordingly, the number of consecutive frost days (CFD, -43.7% / -25.2 days) and the percentage of very cold days (TX10p, -83.4% / -8.13 days) are projected to decrease. The first-time usage of CORDEX-CORE and the larger ensemble size by considering simulations from overlapping domains increase the robustness of the findings from earlier studies. However, some discrepancies in the projected changes prevail among the different RCMs being part of the two CORDEX-domains and in specific landscapes like complex mountainous or lake areas. These uncertainties may be tackled by further model development with improved land-surface processes and potentially higher spatial resolution.

Keywords CORDEX-CORE · Climate extremes · Central Asia · Future projection · Climate change · Model uncertainty

1 Introduction

Various aspects of the climate system are already affected by human-induced climate change. In comparison to earlier time periods, the average surface temperature was much higher in each decade of the last 40 years over the entire globe (IPCC 2021). Climate and weather extremes have been modified due to the increasing global temperature, affecting ecosystems, society, and different economic sectors (Jacob et al. 2018; van Loon et al. 2014). Extreme events and related indices of precipitation and temperature are projected to intensify in the future over different parts of

✉ Praveen Rai
  praveen-kumar.rai@uni-wuerzburg.de

[1] Institute of Geography and Geology, University of Würzburg, Am Hubland, 97074 Würzburg, Germany

[2] Chair of Hydrology and River Basin Management, Technical University of Munich, Munich, Germany

[3] Kinshasa School of Public Health, University of Kinshasa, Kinshasa, Democratic Republic of the Congo

the globe (Bangelesa et al. 2023; Fallah et al. 2023; Ozturk 2023; Paeth et al. 2023; Das and Umamahesh 2022; Liu et al. 2022; Sobie et al. 2021; Kim et al. 2020; Rai et al. 2019). Additionally, global warming will change the atmospheric circulation, resulting in an increased frequency and intensity of (wind) extremes, and will modify the water cycle via altered advection processes and the Clausius-Clapeyron equation (Robinson et al. 2021). Already today, intense extreme events lead to devastating consequences and high death tolls, as exemplified by heat waves in Europe 2003 (D'Ippoliti et al. 2010) and 2018 (Ballester et al. 2023), and Russia 2010 (World Bank 2012), as well as by extreme precipitation, e.g., in Pakistan 2022 (Nanditha et al. 2023). In general, they impact the environment and human population more severely than the change in mean values. Therefore, analyzing how the future climate conditions will affect the occurrence of these extreme events becomes crucial to guide adaptation strategies.

Information on future changes of extreme events is particularly important for the arid Central Asian region located in the heart of Eurasia. This region - which comprises the countries Kazakhstan, Kyrgyzstan, Tajikistan, Turkmenistan, and Uzbekistan - holds one of the most sensitive ecosystems globally (Seddon et al. 2016). The drying of the Aral Sea, the decrease of glacial areas in the Pamir-Alay (Chevallier et al. 2014) and the Tian-Shan mountains (Kenzhebaev et al. 2017), and the increasing population in Kyrgyzstan and Uzbekistan (Pritchard 2017) contribute to the rising water scarcity issues in this region. For Central Asia, a significant warming above global average during the period of 1979–2011 by 0.37–0.43 °C per decade is reported (Yao et al. 2021; Yao et al. 2015). This also affects precipitation extremes, as higher temperatures lead to an increased frequency of heavy rainfall over land areas by 18% in comparison to the pre-industrial period (Fischer and Knutti 2015). While the total precipitation over Central Asia is projected to increase (Chen et al. 2011), a reduction of snowfall acting as an important inter-seasonal water storage is expected (Kraaijenbrink et al. 2021). As a consequence, dry areas have expanded in the last 50 years in Central Asia along with a significant enhancement of temperature extremes and evapotranspiration (Yao et al. 2020, 2021; Luo et al. 2020; Zhang et al. 2017; Hu et al. 2016; Huang et al. 2015). General Climate Models (GCMs) for the whole globe and Regional Climate Models (RCMs) are widely used to project future climate conditions. Earlier studies have used model data from the Coupled Model Intercomparison Project phase 5 (CMIP5) and the state-of-the-art CMIP6 to study the extreme events over Central Asia (Cao et al. 2023; Fallah et al. 2023; Qiu et al. 2023; Dike et al. 2022; Li et al. 2022a, b; Zhang et al. 2019b, 2022; Guo et al. 2021; Yao et al. 2021; Liu et al. 2020). Furthermore, Qiu

et al. (2023) evaluated 22 GCMs and their related dynamically and statistically downscaled products to assess drying trends over Central Asia during historical and future periods. They found significant trends in the past and future towards enhanced dryness, particularly during the boreal summer half year (April-September) being the growing season in Central Asia. Drier conditions during the 21st century based on CMIP6 models were also shown by Cao et al. (2023). Using the bias-corrected and downscaled product from the Inter-Sectoral Impact Model Intercomparison Project (ISIMIP), Fallah et al. (2023) showed an increased likelihood of extreme precipitation especially over the high mountain areas of Kyrgyzstan and Tajikistan together with a higher risk of temperature extremes over large areas of Central Asia. Liu et al. (2020) revealed an increase of 28% of very wet days with reference to the 95th percentile (R95p) and significantly more very hot days at a warming level of 1.5 °C, with a further intensification at 2 °C.

However, the coarse resolution of GCMs used in most of these studies, is a limitation that hinders the representation of important regional processes such as mesoscale circulation, convection and processes along complex topography. Thus, extreme precipitation events are underrepresented in those models (Rummukainen 2010). Dynamical downscaling with RCMs having higher resolutions adds value in representing these processes on the local to regional scale more adequately, leading to a better representation of extreme events - especially extreme precipitation (Gibba et al. 2019). Under the framework of the Coordinated Regional Climate Downscaling Experiment (CORDEX; Giorgi et al. 2009), CORDEX-Coordinated Output for Regional Evaluations (CORE; Giorgi et al. 2022; Gutowski et al. 2016) was launched as a new initiative with a higher resolution of 0.22° covering all global land areas and including more advanced model versions compared to its predecessor. The simulations were run using low and high emission scenarios i.e., Representative Concentration Pathway (RCP2.6 and RCP8.5) (van Vuuren et al. 2011; Moss et al. 2010). The ensembles from CORDEX-CORE represent a dynamical downscaling of the climate change signal from CMIP5 GCMs (Teichmann et al. 2021). They are an appropriate tool for better adaptation, impact, and vulnerability studies (Coppola et al. 2021; Jacob et al. 2020). The simulations from CORDEX-CORE are useful for studying extreme events under future climate across the globe, for example over Africa (Bangelesa et al. 2023; Samuel et al. 2023), South America (Reboita et al. 2022), and India (Maharana et al. 2021). Initially, two sets of RCMs were used in CORDEX-CORE: REMOv2015 (hereafter REMO) (Jacob et al. 2012) and RegCM4 (Giorgi et al. 2012). In the meantime, more modeling centers are participating in generating a larger ensemble in different domains. However, the CORDEX domain of Central Asia

(CORDEX-CAS) is not a priority domain inside the framework of CORDEX-CORE (Giorgi et al. 2022). Hence, only simulations from the RCM REMO (Remedio et al. 2019) and a single run from ALARO-0 (Top et al. 2021) are available for this domain. Our study is among the first to assess extreme events in Central Asia based on CORDEX-CORE.

Our model domain in Central Asia is based on the study region of the European Union funded project "WATER EFFICIENT ALLOCATION IN A CENTRAL ASIAN TRANSBOUNDARY RIVER BASIN (WE-ACT)" which aims at providing a Decision Support System (DSS) for water allocation in a Central Asian transboundary river basin to increase shared benefits and foster the adaptation of water resources management and planning to climate change. Since the available ensemble size from CORDEX-CORE is quite small for CORDEX-CAS (4 simulations), we have also utilized simulations from CORDEX-East Asia (EAS, 6 simulations) covering the area of interest (see Table 1 for the model list and Fig. 1 for the domains). Some artifacts such as border effects and offsets among the ensembles can arise from the overlapping domains that will be considered in the subsequent analysis.

The present study is expected to fill the research gap related to changes in extremes over Central Asia, a generally understudied region within CORDEX-CORE (Remedio et al. 2019; Giorgi et al. 2022), using higher resolved and further developed RCMs compared to the previous CORDEX generation (Teichmann et al. 2021). Despite there are some recent RCM studies focusing on the effect of climate change and extreme events in Central Asia (e.g., Ozturk et al. 2017; Mannig et al. 2018; Ozturk 2023; Russo et al. 2019), the focus of these papers lies on individual models, not an ensemble, with 0.44° resolution. Additionally, our approach of using an overlapping domain to increase the number of ensemble members is a promising (Zittis et al. 2019; Legasa et al. 2020) but rarely used one. Choosing simulations from two domains and building ensembles for each domain as well as showing the behavior of individual simulations, enables us to investigate the effect of domain selection. Therefore, our study provides valuable insights on the development of extreme events in Central Asia based on an ensemble of the latest CORDEX generation. Further, it enhances our understanding of strengths and weaknesses of CORDEX-CORE in representing precipitation and temperature extremes of the ensembles and individual models as they depend on the selected RCM, driving data, and simulation domain.

The paper is organized as follows: The datasets and used methodology are described in Sect. 2. Results are presented in Sect. 3 focusing on the performance of precipitation and temperature simulated by the models, followed by validating the extreme indices for the historical period and examining their changes in the future. The discussion and conclusions are presented in Sects. 4 and 5, respectively.

2 Data and methodology

2.1 Study area

The region of Central Asia is mostly characterized by rain deficit areas with intensive evaporation. It experiences sharp changes in temperature from season to season and spatially from grasslands to temperate deserts (Zhang et al. 2019a). The study domain covers the lowlands of Turkmenistan and Uzbekistan in the West and of Kazakhstan in the North as well as the Chinese Province Xinjiang with the Taklamakan desert in the East. It further covers the high mountain ranges of Pamir, Tian Shan, and the Himalaya as well as parts of the Tibetan Plateau which spread along Kyrgyzstan, Tajikistan, parts of Xinjiang, Afghanistan, Pakistan, and India. Extratropical westerlies and orographic lifting (Barlow and Tippett 2008) govern the precipitation pattern in this orography-dominated region, ranging from 50 to 1000 mm per year. The Indian summer monsoon also affects a part of the central and eastern Tian Shan as well as Pamir's south-eastern flank (Meier et al. 2013). The CORDEX-CAS and CORDEX-EAS domains are shown in Fig. 1a. The location and orography of the CEAS is shown in Fig. 1a and b, respectively. The WE-ACT project aims to develop a Decision Support System (DSS) for water allocation in a Central Asian transboundary river basin to increase shared benefits and foster the adaptation of water resources management and planning to climate change and further investigate the effects of irrigation in catchments of tributaries of the Syr Darya river using climate and hydrological models. Thus, the selected CEAS-domain builds upon the work of Rai et al. (2022), who applied an interactive vegetation module for Central Asia. Subsequent development steps, such as the implementation of a more advanced soil hydrology (Abel 2023) and an irrigation scheme (Rai et al. 2023), are currently underway.

2.2 CORDEX-CORE simulations

The present study considers simulations from CORDEX-CORE having a horizontal resolution of 0.22° x 0.22° and a more advanced development stage of the RCMs compared to its predecessor runs with 0.44° x 0.44° resolution. This is advantageous to simulate land surface processes, meso-scale atmospheric circulation and synoptic features, especially in complex mountainous regions within our study domain. The Central Asian ensemble from CORE (ENS_CAS), however, only consists of four members. To enlarge the entire

a)

b)
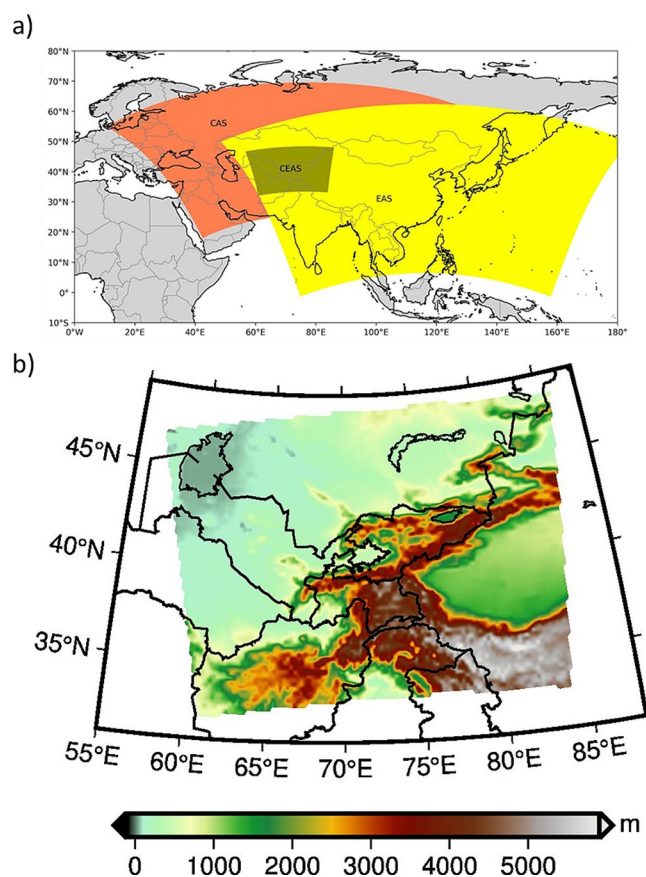
Fig. 1 (**a**) The spatial extent of the two CORDEX domains CAS (orange rectangle) and EAS (yellow rectangle) from which simulations have been used, and of our selected overlapping area (grey rectangle), (**b**) the topography of our study region (data source: GTOPO30)

ensemble size, we further consider the East Asian ensemble (ENS_EAS with six members). Details of the used model simulations are presented in Table 1. A detailed overview of the settings used for the CORDEX-CORE simulations is provided by Diez-Sierra et al. (2022a).

This enables the analysis of the overlapping domain and of potential effects on the simulated climate due to different distances to the domain boundaries. Zittis et al. (2019) and Legasa et al. (2020) compared simulations from overlapping

domains for the Legasa et al. (2020) found that most of the variance is introduced by the selected models while the domain choice only accounts for a small part of the variance which exceeds the one of the model selection solely locally. Thus, they conclude that simulations from different domains are transferable. The historical experiments span the time range from 1981 to 2005 caused by the availability of model data before 1981 and differing scenarios from 2006 onwards. In CORDEX-CORE, only two scenarios, RCP2.6 and RCP8.5, are available. For future runs, we use RCP8.5 covering two periods (2031–2055 as near-future, and 2071–2095 as far-future) to investigate long-term future changes of extreme events. We have chosen the RCP8.5 scenario as it follows a high impact pathway and, thus, enables the analysis of the assumed maximum limit of climate change in the study region. A flowchart of the model combinations and the domains covered is shown in Fig. 2, which highlights the analysis of all three ensembles (ENS, ENS_CAS, and ENS_EAS) for projecting precipitation and temperature extremes and also account for the potential issues arising from this partly inconsistent ensemble from two different domains.

2.3 Validation datasets

For validating simulated mean precipitation and related indices, we used the latest version of the Multi-Source Weighted-Ensemble Precipitation (MSWEP v2.8; Beck et al. 2019; Beck et al. 2017a, b) data, having a horizontal resolution of 0.1°. MSWEP is a widely used, global, and gridded precipitation product that merges various gauge-, satellite-, and reanalysis-based datasets and, thus, combines the strengths of the individual datasets (Beck et al. 2019) as it is recommended, e.g., by Prein and Gobiet (2017). To effectively match the rain gauge observations, no corrections have been applied in this version regarding the underestimation of precipitation in mountainous and snow dominated regions (Beck et al. 2021). The accuracy of MSWEPv2 is improved compared to v1 because of the introduction of the cumulative distribution function and the precipitation

Table 1 List of used simulations from CORDEX-CAS and CORDEX-EAS

RCMs	Domain/Resolution	Driving GCMs	References
REMO2015.v1	CAS/0.22° (Daily)	MOHC-HadGEM2-ES MPI-M-MPI-ESM-LR NCC-NorESM1-M	Jacob et al. 2012; Remedio et al. 2019; Giorgi et al. 2022
ALARO-0.v1		CNRM-CERFACS-CNRM-CM5	Top et al. 2021
REMO2015.v1	EAS/0.22° (Daily)	MOHC-HadGEM2-ES MPI-M-MPI-ESM-LR NCC-NorESM1-M	Jacob et al. 2012; Remedio et al. 2019; Giorgi et al. 2022
RegCM4-4.v0		MOHC-HadGEM2-ES MPI-M-MPI-ESM-MR NCC-NorESM1-M	Giorgi et al. 2012; Giorgi et al. 2022

Fig. 2 Flowchart depicting available simulations of the different CORDEX domains used for our ensembles and index calculations for different time periods
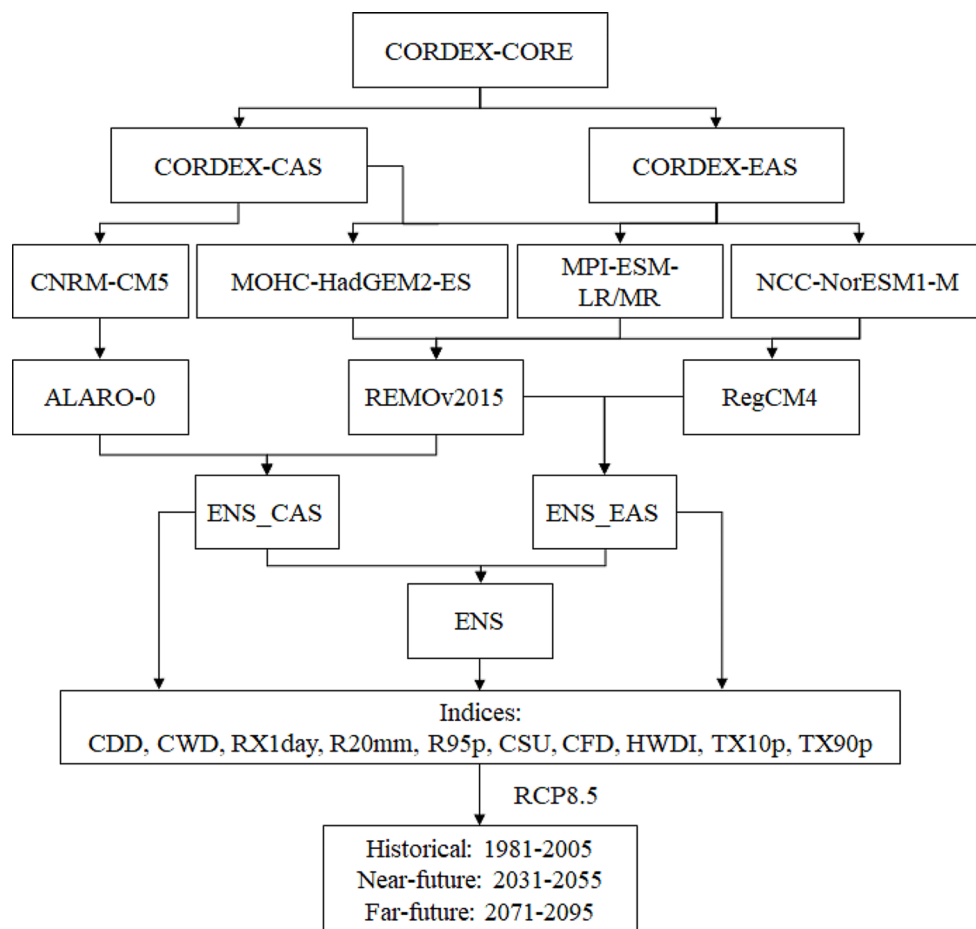
frequency (Beck et al. 2021). MSWEP excels with respect to the correlation coefficient of precipitation with measurements taken from rain gauge stations on various temporal scales over Central Asia especially during winter and spring (Peña-Guerrero et al. 2022). Li et al. (2022b) also observed a good performance of MSWEP in capturing positive and negative precipitation changes and drought characteristics. The MSWEP precipitation data was downloaded from the official website https://www.gloh2o.org/mswep/ (accessed on 29 April 2022).

For the validation of maximum, minimum, and mean temperature, and related indices, we used the European ReAnalysis Land (ERA5-Land: 0.1°; Muñoz-Sabater et al. 2021) data from the European Centre for Medium-Range Weather Forecast (ECMWF). In comparison to the predecessors ERA5 and ERA-Interim, having coarser resolutions than ERA5-Land (35 km and 80 km vs. 9 km, respectively), an added value has been observed in the representation of the hydrological cycle by using the more advanced land surface scheme (Carbon Hydrology-Tiled ECMWF Scheme for Surface Exchanges over Land (CHTESSEL) (Boussetta et al. 2013). Examining ERA5 and ERA5-Land, Xu et al. (2022) and Zhao et al. (2023) found that these reanalyses

are able to capture temperature and derived indices on the Tibetan Plateau and in the Qilian Mountains regarding their absolute value and trend. We did not consider ERA5-Land for the precipitation indices as the number of precipitation events is significantly overestimated, causing strong biases for wet and dry periods (Abel et al. 2024b).

2.4 Extreme indices and evaluation metrices

Extreme climate indices from the Expert Team on Climate Change Detection and Indices (ETCCDI; Zhang et al. 2011) have been widely used in earlier studies (e.g., Paeth et al. 2023; John et al. 2022; Rai et al. 2019). In the current study, we selected five indices based on precipitation (CDD, CWD, RX1day, R20mm, and R95p) and temperature each (CSU, CFD, HWDI, TX10p, and TX90p). CDD, CWD, CSU, and CFD indicate the duration, while R95p, HWDI, TX10p, and TX90p are percentile-based indices. As a threshold-based index, we consider R20mm. These indices act on an annual scale to obtain comparability with existing studies focusing on these indices using GCM ensembles or RCMs. The indices are presented with their corresponding description and unit in Table 2.

Table 2 Analyzed extreme indices for precipitation and temperature

Abbreviation	Definition of the index (based on Zhang et al. 2011; Schulz-weida 2019)	Unit	Input Variable
CDD	Consecutive dry days index per year (with Pr < 1 mm for more than 5 days)	days	Pr
CWD	Consecutive wet days index per year (with Pr ≥ 1 mm for more than 5 days)	days	Pr
R20mm	Very heavy precipitation (Pr ≥ 20 mm) days index per year	days	Pr
RX1day	Highest one day precipitation amount per year	mm	Pr
R95p	Very wet days percent per year w.r.t. 95th percentile of reference period (1981–2005)	% of days	Pr
CSU	Consecutive summer days index per year (with T_{max} > 25 °C for more than 5 days)	days	T_{max}
CFD	Consecutive frost days index per year (with T_{min} < 0 °C for more than 5 days)	days	T_{min}
HWDI	Heat wave duration index per year w.r.t. mean of reference period (1981–2005)	days	T_{max}
TX10p	Very cold days percent per year w.r.t. 10th percentile of reference period (1981–2005)	% of days	T_{max}
TX90p	Very warm days percent per year w.r.t. 90th percentile of reference period (1981–2005)	% of days	T_{max}

For a better comparison, all datasets are remapped on the common CORDEX-CORE grid of the CAS domain with 0.22° x 0.22° resolution using a bilinear interpolation. To validate the model data, the spatial bias patterns are calculated with respect to MSWEP for precipitation and to ERA5-Land for maximum, minimum, and mean temperature. We have calculated the indices for each GCM-RCM pair and generated all three ensembles afterwards. The standardized standard deviation (SSD) along with the spatial correlation coefficient for extreme indices of each individual simulation as well as for ENS, are also presented in heatmaps. The standardization is achieved by dividing the spatial standard deviation of individual RCMs by the spatial standard deviation of the validation data. Therefore, SSD values close to 1 indicate a close proximity to the standard deviation of the respective observation dataset. Within a heatmap, we ranked the best three simulations based on their performance. The probability distribution function (PDF) is also calculated for all three ensembles' indices and compared with the PDFs of the validation data.

Projected changes of extreme indices are calculated relative to the historical period of 1981–2005 by dividing the difference of the future and past value by the past value. The

long-term change was considered reliant only when ~ 70% of the models (7 out of 10 for ENS, 3 out of 4 for ENS_CAS, and 4 out of 6 for ENS_EAS) agree on the direction of change following the approach used in Bangelesa et al. (2023) and Spinoni et al. (2021, 2020). We also calculate area-averaged indices over the entire domain and present the results in a box and whisker plot showing the variability and distribution of the long-term changes.

3 Results

3.1 Precipitation and temperature climatology

3.1.1 Precipitation

The spatial pattern of the climatological daily precipitation from MSWEP and the relative biases of each individual simulation and the ensembles compared to MSWEP are presented in Fig. 3 during the 1981–2005 period. Regarding the bias patterns, it has to be noted that the study area shows a wide range of precipitation amounts with high windward mountain ranges (e.g., Karakoram) and deserts (e.g., Taklamakan). Thus, the relative biases have to be treated with caution. The corresponding absolute biases of the ensembles, individual RCMs, and driving GCMs are plotted in Figure S1.

The observations show higher precipitation values in mountainous regions that are mainly located in the eastern and southern part of the domain (Fig. 3a). Spatial variability is enormous, spanning from below 0.5 mm/day in the arid lowlands to more than 3.5 mm/day along the high mountain chains. ENS shows wet biases in the orographically complex regions of Kyrgyzstan and Tajikistan and the areas south of it, while the western and northern arid lowlands of the domain have either a small dry or no bias (Fig. 3b). These bias patterns are quite similar in ENS_CAS and ENS_EAS. However, ENS_CAS shows a lower (higher) magnitude for the wet (dry) biases in high-elevation (lowland) regions (Fig. 3c) compared to ENS_EAS (Fig. 3d). For individual simulations, the ALARO-0 model forced with CNRM-CM5 from CORDEX-CAS (Fig. 3h) shows the lowest biases among all simulations (excluding the Taklamakan, see absolute bias in Figure S1) while RegCM4 from CORDEX-EAS exhibits the largest biases independent of the driving GCM (Fig. 3l-n). A recent study by Top et al. (2021) found a better representation of precipitation patterns in ALARO-0 compared to REMOv2015 over Central Asia. Earlier studies have also reported a general precipitation overestimation of RegCM over China (Gao et al. 2017), and over topographic regions of Central Asia (Guo et al. 2021; Ozturk et al. 2017, 2012; Oh et al. 2014; Park et al. 2013; Giorgi

Fig. 3 Climatology of mean daily precipitation (mm/day) for (**a**) MSWEP, and relative biases of the ensembles (**b–d**) and single simulations in comparison to MSWEP from CORDEX-CAS (**e–h**), and CORDEX-EAS (**i–n**) for the period of 1981–2005
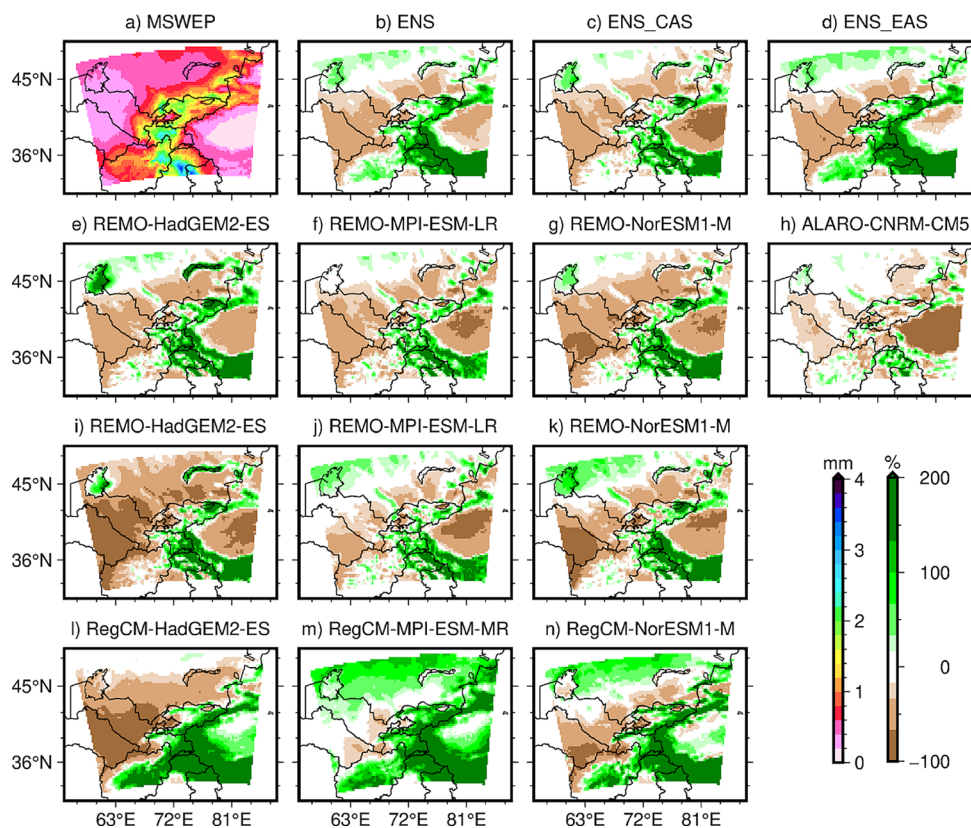

et al. 2012). The RCM REMO forced with MPI-ESM-LR from both CORDEX-CAS and EAS (Fig. 3f and j) captures the precipitation pattern better compared to forcings from HadGEM2-ES and NorESM1-M (Fig. 3i, l and k, n, respectively). Driven by HadGEM2-ES, the REMO runs of EAS show a more prominent dry bias in the northern and western parts of CEAS than the runs of CAS (Fig. 3e, i) and an opposite behavior when REMO is forced with the other two GCMs (Fig. 3f-g, j-k). This is a clear effect of the forcing data which has also been found by Oh et al. (2014) using HadGEM2 and by Park et al. (2013) comparing the effect of different boundary conditions on RegCM4. Focusing on the absolute values (Figure S1), RegCM has the strongest bias patterns while REMO and ALARO-0 show lower biases compared to the respective forcing data and, thus, are adding value to these simulations. This further is remarkable due to the strong biases HadGEM2-ES produces over the Taklamakan which are clearly reduced in REMO and RegCM4. In general, the bias patterns in CEAS are strongly orography-driven as all models are limited by their spatial resolution and the resulting inability to represent the actual topographical heterogeneity. This has been reported earlier by Rai et al. (2022), Top et al. (2021), and Russo et al. (2019) who focus on single models instead of ensembles. Beside different topographical input datasets (GTOPO30 for REMO and RegCM4 (Giorgi et al. 2022; Ziegler 2022; Jacob et al. 2012) and GMTED2010 for ALARO (Termonia et al.

2018), used model grids, and applied interpolation methods, all three RCMs use different convection schemes (MT3 in ALARO-0 (Top et al. 2021), Tiedtke in REMO (Remedio et al. 2019), Emanuel in RegCM4 (Diez-Sierra et al. 2022a) and different numbers of vertical layers (47 in ALARO-0 (Top et al. 2021), 27 in REMO (Giorgi et al. 2022), 23 in RegCM4 (Giorgi et al. 2022). The good performance of precipitation in ALARO-0 could be caused by the more detailed vertical resolution of the atmosphere. However, the distinct attribution of individual bias causes is beyond the scope of the study.

3.1.2 Mean temperature

When looking at the climatology and bias patterns of the 2 m mean temperature, one can observe the orographic and latitudinal dependence in ERA5-Land (Fig. 4a). ENS (Fig. 4b) is characterized by warm biases in the central and northern part and by cold biases in the southern parts and the Tibetan Plateau, while a more scattered bias pattern dominates the mountain areas. The magnitude of biases is quite small in ENS_CAS, which mostly shows a cold bias in Kyrgyzstan and the areas south of it (Fig. 4c), while medium to strong warm biases cover most areas in ENS_EAS (Fig. 4d). Focusing on individual simulations, REMO from both CORDEX domains outperforms the other runs (Fig. 4e-g and i-k). Nevertheless, the effect of the forcing data in producing a

Fig. 4 Climatology of mean daily 2 m mean temperature (°C) for (**a**) ERA5-Land, and biases of the ensembles (**b**–**d**) and single simulations in comparison to ERA5-Land from CORDEX-CAS (**e**–**h**), and CORDEX-EAS (**i**–**n**) for the period of 1981–2005
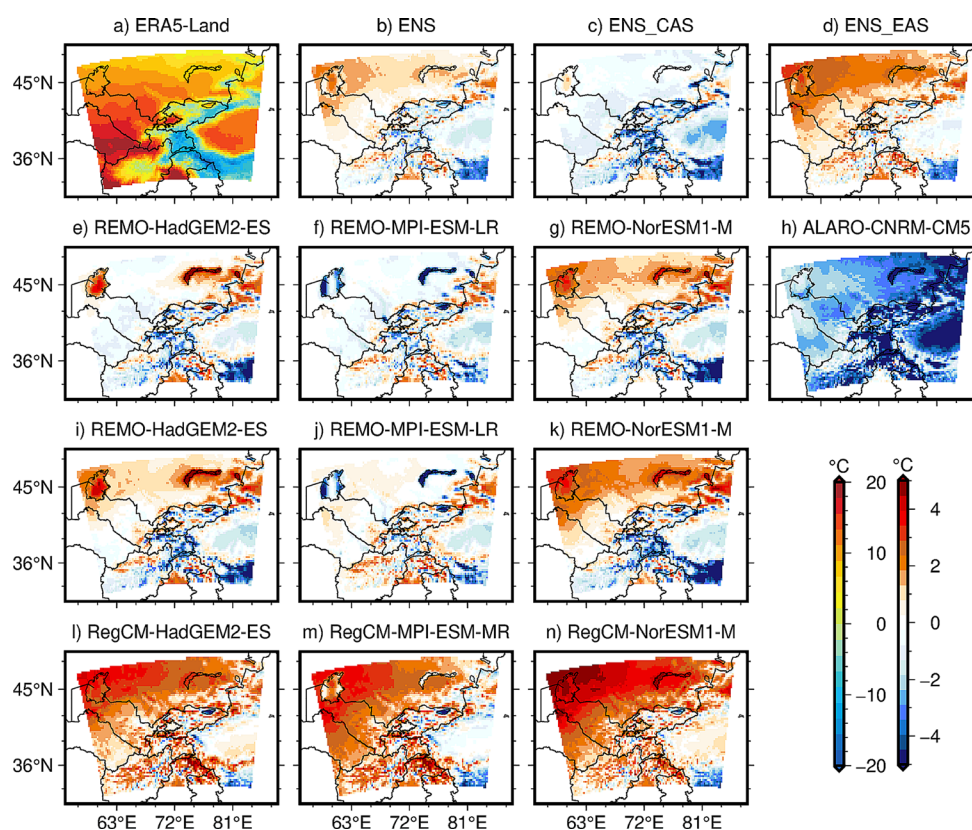
systematic warm bias in the northern part is evident in the NorESM1-M-driven runs and, to a lower extent, the Had-GEM2-ES-driven ones. The good performance of REMO in capturing temperature patterns over Central Asia is also confirmed by earlier modeling studies (Rai et al. 2022; Top et al. 2021; Mannig et al. 2013). ALARO-0 is marked by a strong and systematic negative bias which mostly arises from winter and spring seasons where the model's single-layer does not simulate the snow cover accurately - other than REMO's multi-layer snow scheme (Top et al. 2021). A strong warm bias over large parts of the domain except the southeastern part is present in all simulations of RegCM4 and has been previously described and linked to the model's multi-layer snow-scheme by Ozturk et al. (2012). Although the driving data affect the biases' magnitude, this RCM obviously exhibits a systematic warm bias. All RCMs show limitations of the temperature simulation in lake areas (e.g., Aral Sea, Lake Balkhash) where the sign of the bias depends on the driving data. In a more recent version of REMO, which has not been used in CORDEX-CORE, an advanced lake model has been implemented resulting in a reduction of temperature biases in lake areas of Fenno-Scandinavia (Pietikäinen et al. 2018).

3.1.3 Maximum and minimum temperature

The spatial bias patterns for maximum and minimum temperatures in reference to ERA5-Land are presented in Supplementary Figs. S2 and S3, respectively. The general bias patterns are comparable to the ones of the mean temperature, but the magnitude of the biases differs among the models. Nearly all simulations show an overestimation of the maximum temperature in mountain regions, except for ALARO-0, which shows an underestimation similar to its mean temperature (Fig. S2). An underestimation of the minimum temperature can be seen over the orographic parts in most of the simulations (Fig. S3). However, the REMO simulations show an underestimation of the minimum temperature and an overestimation of the maximum temperature in the high mountain areas which, thus, is not caused by the different domains or driving GCMs. Although this behavior is not typical for climate models, which tend to underestimate the daily temperature range (Wang and Clow 2020; Lindvall and Svensson 2015) the same finding has also been reported by Top et al. (2021). However, Rai et al. (2022) found an overestimation of minimum temperature in the mountain areas. The differences might be attributed to different forcing data, examined periods, validation data, different spatial resolutions, or a combination of these effects. There is also uncertainty in gridded validation products, especially in complex orographic regions (Russo et al. 2019) and where

an inaccurate representation of snow cover may lead to an overestimation of minimum temperature (Mašek 2017).

3.2 Extreme indices during the historical period

Figure 5 shows the spatial correlation coefficients between the respective observations and the individual simulations as well as ENS for the extreme precipitation and temperature indices. High coefficients can be observed for CDD and R95p as precipitation indices and for CSU and CFD as temperature indices. Except for R95p, for which ALARO-0 performs best, for all these indices ENS is the overall best

performer especially for the temperature indices. Among individual simulations, ALARO-0 performs best in representing the precipitation indices followed by REMO-MPI-ESM-LR from CORDEX-CAS. Generally, high correlations can be observed for REMO-HadGEM2-ES from both CORDEX domains compared with the same GCM forcing for RegCM4. Low correlation coefficients occur for precipitation indices which are related to wet conditions such as CWD, R20mm, and RX1day. The percentile-based indices for temperature extremes (HWDI, TX10p, and TX90p) show lower correlation coefficients as well. Thus, the simulated spatial occurrence of heat waves and cold spells differs

Fig. 5 Spatial correlation coefficient between the ENS and each model with the corresponding validation data for the reference period of 1981–2005 per index. Numbers within the boxes indicate the three best performing simulations for each index
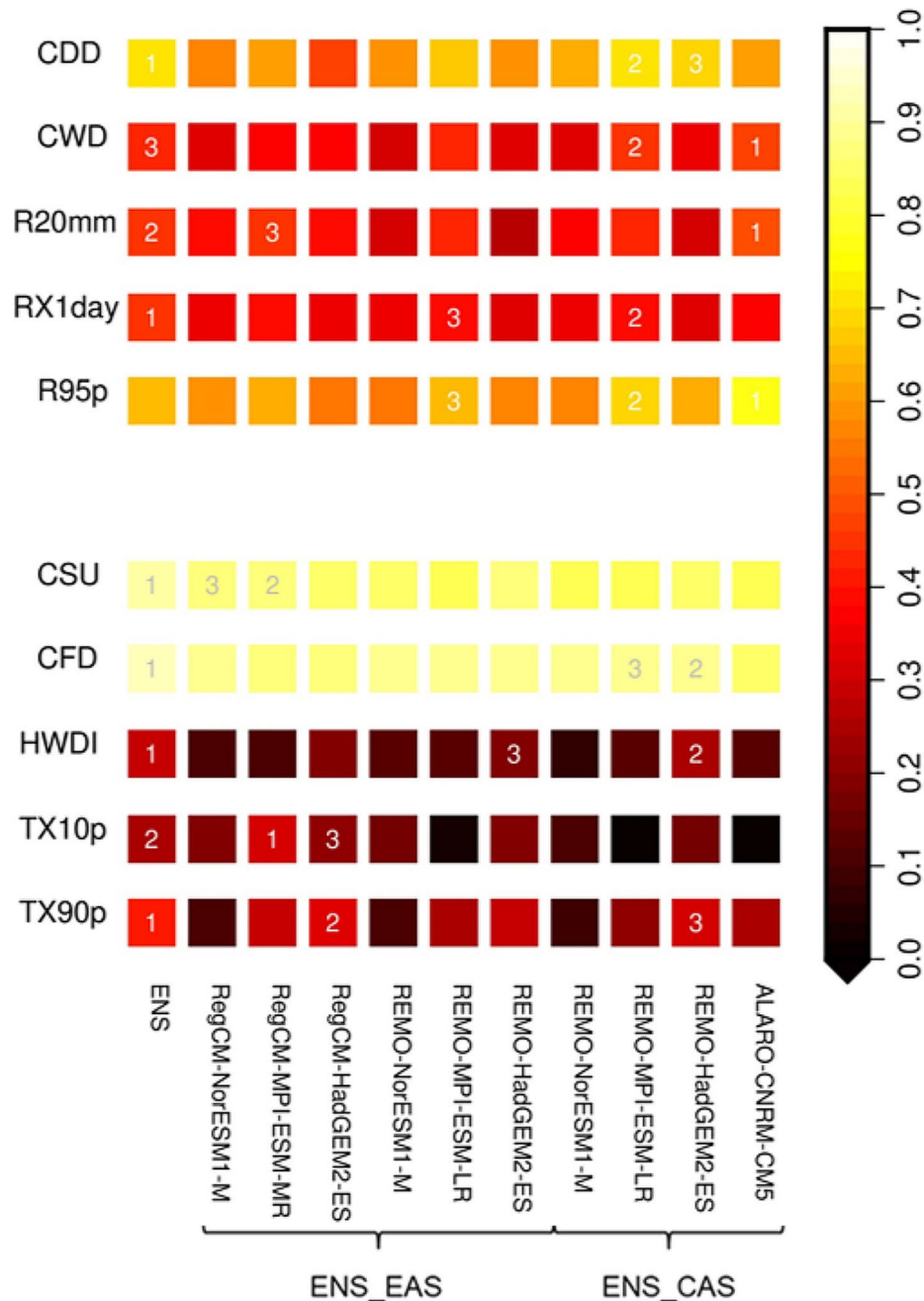
from the one of ERA5-Land. However, ENS shows the best results in this regard.

The bias patterns of the precipitation indices in comparison to MSWEP are presented in Supplementary Fig. S4 for all three ensembles. The overestimation of CDD over the northern part of the domain is consistent among the ensembles while the southern parts are mostly marked by an underestimation (Fig. S4b and c). For wet precipitation indices (CWD, R20mm, RX1day, and R95p), there is a general overestimation in mountainous regions (Fig. S4d-o), particularly in ENS_EAS, which is accompanied by an underestimation in the lowlands. For temperature indices, CSU is slightly overestimated in the lowlands by ENS_EAS (Fig. S5c) while ENS_CAS is marked by an underestimation in these areas (Fig. S5b). Regarding CFD, ENS_CAS shows a systematic overestimation in the Southeast and at high elevations while ENS_EAS mostly underestimates this index (Fig. S5d-f). Focusing on HWDI, the three ensembles are more in line with each other showing strong overestimations in the Taklamakan desert and the western lowlands. The biases in the orographic regions are differing among the ensembles depending on the specific location but with a consistent overestimation in ENS_CAS (Fig. S5g-i). The bias patterns of the percentile-based indices TX10p (Fig. S5j-l) and TX90p (Fig. S5m-o) are dominated by noise caused by the calculation method of these two indices.

The spatial SSD between each GCM-RCM pair and their ENS compared to MSWEP and ERA5-Land, respectively, is shown in Fig. 6 for the ten indices. Focusing first on precipitation indices, CDD, RX1day, and R95p mostly show a too low SSD. While the SSD of R20mm is mostly overestimated, CWD shows a more diverse picture depending on the RCM and the driving data with RegCM4 and forcing by HadGEM2-ES having a tendency towards higher SSDs. There is not a clear individual model or ensemble outperforming the others. However, when driving an RCM with NorESM1-M, generally good ranks are achieved. We have to note that none of the models is able to simulate all indices with a good agreement of SSD with the spatial standard deviation of MSWEP. In the case of the temperature indices, all simulations underestimate the standard deviation of ERA5-Land. For TX90p, TX10p, and HWDI, however, ENS and ALARO-0 show the best representation. Regarding CFD, REMO has a generally better SSD independent of the driving data. In contrast to precipitation, the SSDs from the temperature indices have a lower dependency on the driving data and a higher on the individual RCM behavior.

The PDFs based on the spatial distribution of the ensemble-mean precipitation and temperature indices in comparison to the respective observational dataset are shown in Figs. 7 and 8, respectively. For precipitation, the distributions are mostly too narrow (e.g., CWD, RX1day)

compared to MSWEP. Some ensemble PDFs show no or a quite small overlapping value range with the validation data (e.g., CWD, R20mm). Thus, the observed spatial means and extremes are not captured by the models. The best performing ensemble strongly depends on the considered index (e.g., CDD, CWD). As shown in Fig. 3, ENS_CAS generally demonstrates drier conditions than ENS_EAS. This originates from the high precipitation amounts simulated in RegCM4, which tends to show not only higher precipitation amounts (Fig. 3) but also a higher frequency (Fig. 7a, b for CDD, CWD) and intensity (Fig. 7c, e for R20mm, R95p). Generally, the PDFs of ENS_CAS fit better than the ones of ENS, both of which are outperforming ENS_EAS. Only for RX1day the three ensembles are close to each other and MSWEP (Fig. 7d). Considering the temperature indices (Fig. 8), the ensemble PDFs match generally better with the validation data from ERA5-Land. However, the spread is mostly too narrow as indicated by the SSDs as well. While HWDI, TX10p, and TX90p are quite similar in the ensembles, differences between the regions can be seen for CSU and CFD (Fig. 7c-e). Here, ENS_CAS demonstrates a lower spread of the temperatures since CSU is under- and CFD overestimated.

3.3 Projected changes of the climate indices

3.3.1 Precipitation indices

The long-term projected changes of the precipitation indices for the near- and far-future are presented in Figs. 9 and 10, respectively. All changes are shown relative to the historical period.

CDD In terms of CDD during near-future (Fig. 9a-c), ENS simulates more dry days in the northern and north-western parts, while the eastern parts are expected to experience a reduced number of CDDs (Fig. 9a). ENS_CAS projects a shorter dry period of around 10% in the near-future over the northern and eastern part of the domain (Fig. 9b). Approximately 70% of the model simulations agree on the sign of change. In contrast, ENS_EAS estimates longer dry periods during the middle of the century which spread over most parts of the domain except for the southern and easternmost areas (Fig. 9c). While the majority of the models indicate the same sign of change in ENS_EAS, this implies that, in combination with ENS_CAS, ENS shows sign agreements only at a few grid points. In the case of CDD's far-future, the spatial patterns of ENS are expected to remain the same, but their magnitude will intensify substantially (Fig. 10a-c). ENS_EAS (Fig. 10c), in particular, projects an increase of more than 30% of CDD over a large part of the domain, but not in Xinjiang where a decrease is expected at the end

Fig. 6 Standardized spatial standard deviation (SSD) between the ENS and each model with the corresponding validation data for the reference period of 1981–2005 per index. Numbers within the boxes indicate the three best performing simulations for each index
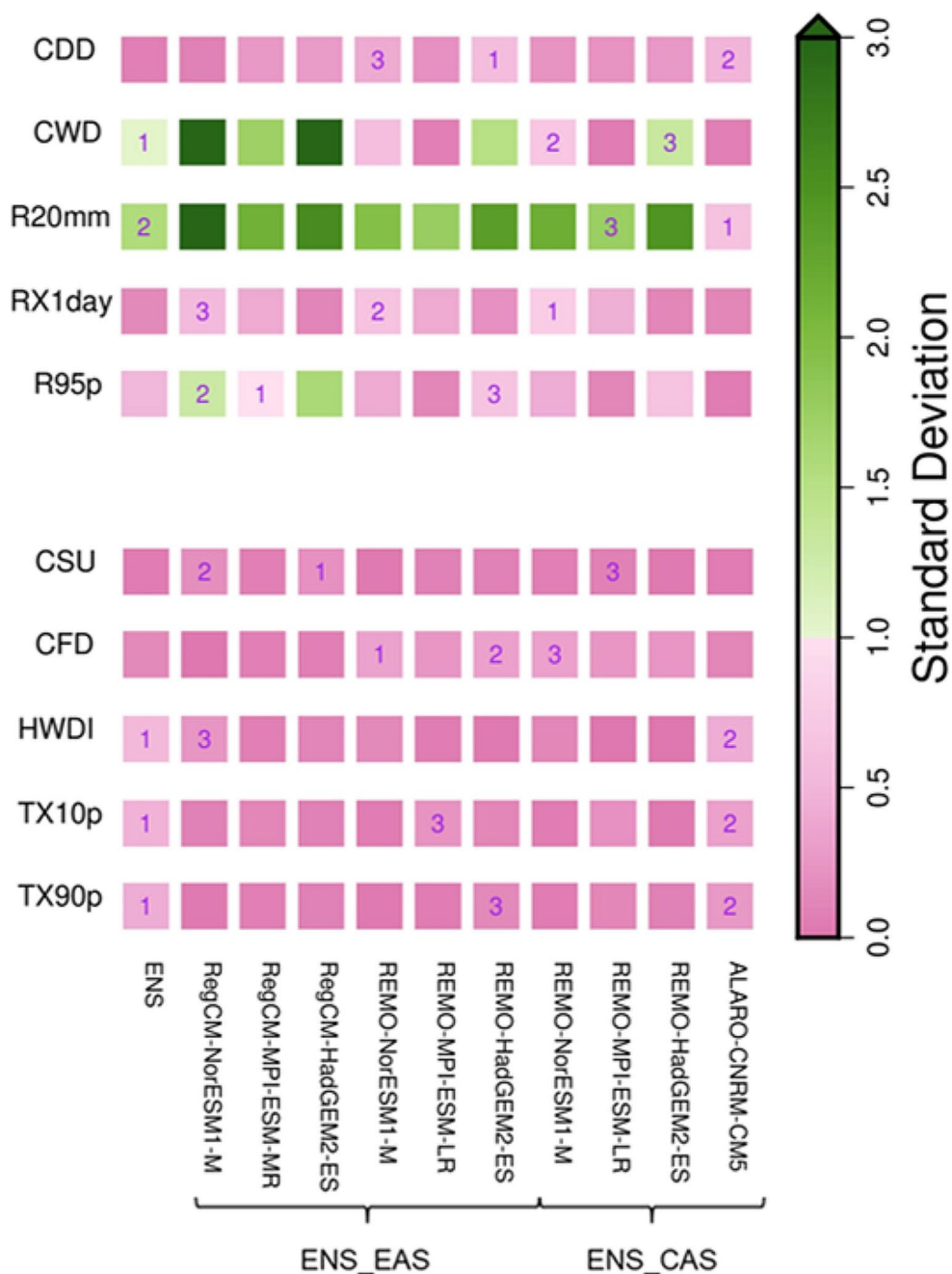

of the century. Thus, while some areas exhibit no change or a reduction during the near-future, large parts of these areas show an increase now as well. This results in a higher percentage of sign agreement among the models visible in ENS. For a historical period (1957–2005), Zhang et al. (2017) found a decreasing trend of CDD over Central Asia using daily climate observations from 55 meteorological stations. Examining the future, a recent study by Ozturk (2023) using RegCM4.3.5 at 0.5° x 0.5° resolution forced by HadGEM2-ES and MPI-ESM-MR pointed to a decrease in CDD, especially over Uzbekistan and Turkmenistan, under RCP8.5. Having these studies in mind, it must be

concluded that a large uncertainty on the change of CDD prevails among the models.

CWD Focusing on CWD, the central part of the domain is projected to experience an increase in the near-future as indicated by all three ensembles. However, the change patterns are not entirely consistent, especially in ENS_CAS (Fig. 9e). Over the southern parts, a significant decrease of CWD is simulated (Fig. 9d-f) which is expected to intensify and expand further northwards towards the end of the century (Fig. 10d-f). Looking at the direction of change, there is no agreement in most parts of the domain. For the far-future

Fig. 7 PDFs of the precipitation indices for the reference period (1981–2005)
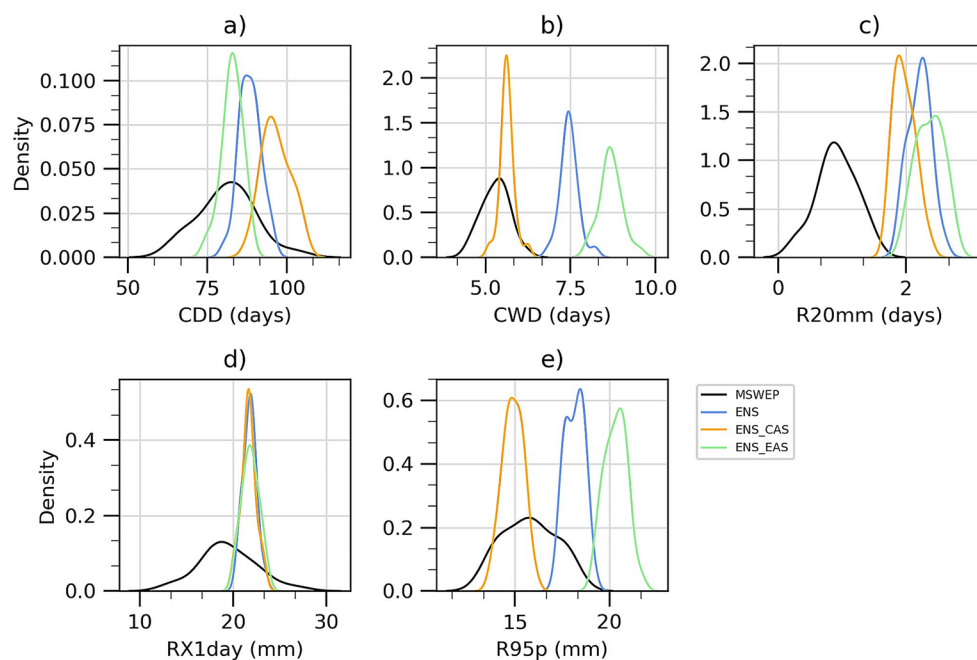
Fig. 8 PDFs of the temperature indices for the reference period (1981–2005)
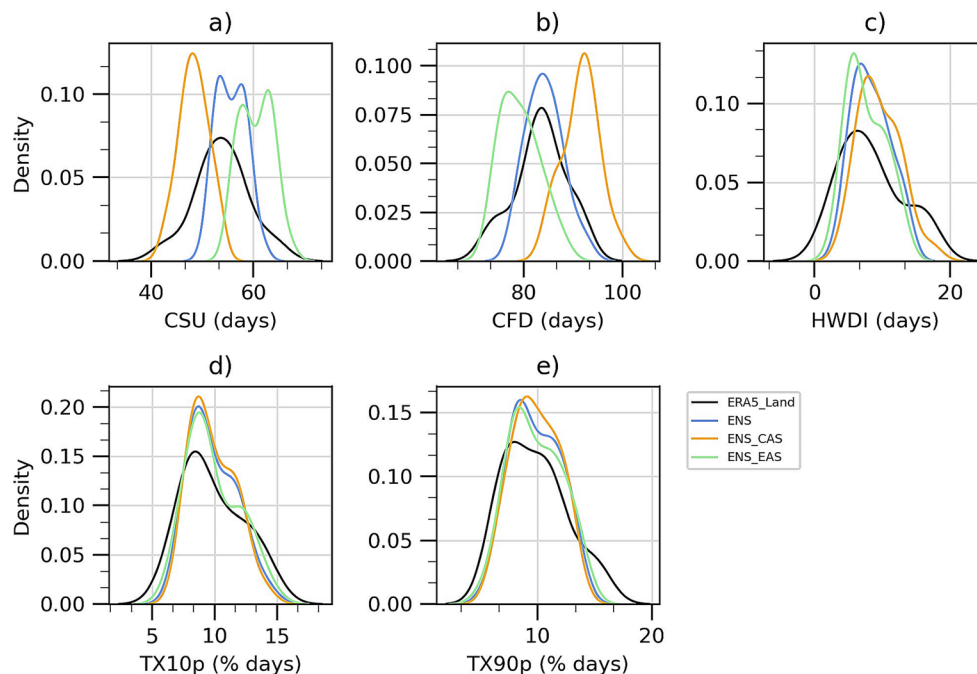
and in comparison with CDD, there are areas showing an increase of both indices. This points in the direction of a more pronounced seasonality of precipitation or more persistent weather types leading to consecutive dry or wet days.

R20mm The projected changes of R20mm, referring to heavy rainfall days, show a clear rise over nearly the entire area for both time periods and with higher intensity at the end of the century (Fig. 9g-i). However, the most significant change, where a majority of the simulations agree on

its sign, is primarily confined to the orographically complex areas of Kyrgyzstan, Tajikistan, and the North of Pakistan. Some parts of the Taklamakan desert in China indicate a slight decrease or no change of this index during the middle of the century (Fig. 9h), but these areas are also expected to experience a growing number of very heavy precipitation days by the end of the century (Fig. 10g-i). A projected

increase of R10mm was also found in the studies by Ozturk (2023) and Zhu et al. (2020).

RX1day RX1day is of significant importance due to its linkage to very extreme precipitation events with potential damage. A significant increase of more than 20% over the entire domain, with stronger increases in orographic regions and northern areas, is simulated consistently throughout the ensembles (Fig. 9j-l). Furthermore, all three ensembles agree on a further intensification under climate change which is consistent among the majority of model simulations by the end of the century (Fig. 10j-l).

R95p Finally, R95p shows an increase in Xinjiang and Kyrgyzstan while the southern parts of the domain are showing a decrease of appr. 10% (Fig. 9m-o). Again, the magnitude of these changes intensifies in the far-future (Fig. 10m-o). However, there are diverging behaviors for Kazakhstan depending on the ensemble. Here, ENS_EAS anticipates a

slight decrease in northern and no changes of R95p in central areas during the middle of the century (Fig. 9o). In contrast, ENS_CAS projects a slight increase in similar regions (Fig. 9n). Interestingly, many areas with a decrease of R95p correspond with the decrease in CWD. These findings are consistent with the study of Zhang et al. (2020), who used the Community Earth System Model (CESM) to project extreme indices for 1.5 and 2 °C warming levels and found an increase of RX1day and R95p over the East of Central Asia.

Summary Overall, a robust increase among the models is projected for R20mm, RX1day, and CDD (Fig. 9). The projected changes have an inhomogeneous pattern in the case of CWD and R95p. Although precipitation extremes are projected to increase further towards the end of the century

Fig. 9 Projected changes of precipitation indices [%] from ENS (left column), ENS_CAS (center), and ENS_EAS (right) for the near-future (2031–2055) compared to the reference period (1981–2005). Stippling denotes grid points where more than 70% of the simulations agree on the sign of change
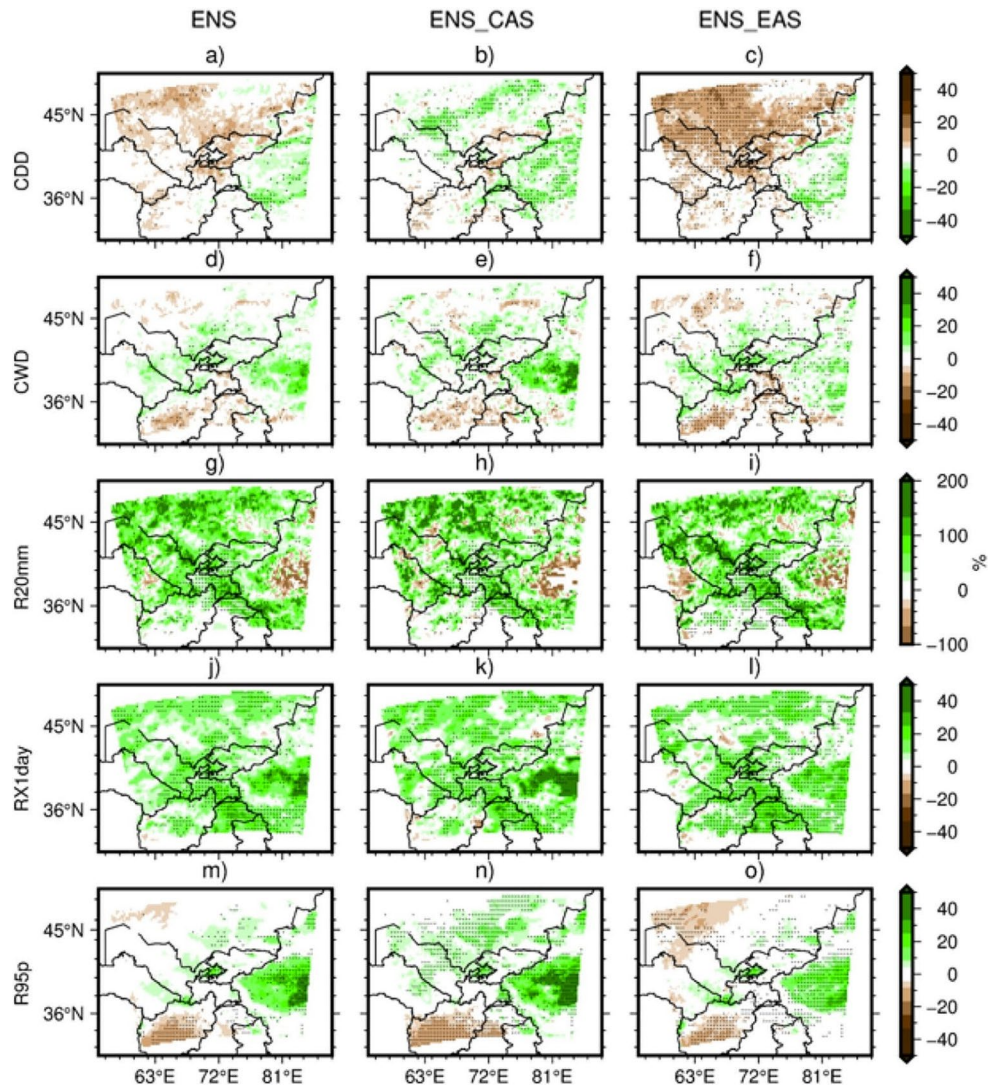
(Fig. 10) over a large part of the domain, the mountainous regions are going to be affected most.

In Fig. 11, the area-average of the precipitation indices' relative change for both time periods are shown using box and whisker plots (for absolute changes see Fig. S6). There are significant discrepancies in the projections of CDD and CWD between the ENS_CAS and ENS_EAS ensembles, as illustrated in Fig. 11a and b and already noted in the context of Figs. 9 and 10. The most pronounced increase, which is expected to further intensify by the end of the century, is observed for R20mm (Fig. 11c). Note that an increase of about 100% is projected which implies a doubling of heavy precipitation events compared with the historical period. A similar change pattern is also observed for RX1day, although with a lower magnitude (Fig. 11d). It is noteworthy that, regarding R20mm and RX1day, all three ensembles agree in the direction as well as the magnitude of change with only slight differences regarding the distributions of the individual ensembles. Regarding R95p, ENS_CAS

projects a moderate increase, while ENS_EAS estimates a slight increase or no change, as indicated in Fig. 11e. Nonetheless, the spatial heterogeneities revealed in Figs. 9 and 10 should be considered.

### 3.3.2 Temperature indices

Shifting the focus to the projected changes in extreme temperature indices, Figs. 12 and 13 illustrate the spatial patterns for the near- and far-future, respectively. The changes are again shown in percentage with respect to the historical period. It is important to note that the indices show an undirectional nature of change. Thus, there are no uncertainties regarding the sign as it is the case for precipitation indices.

CSU Before looking at the changes in CSU, it has to be noted that the high mountain areas are masked as the index is based on an absolute temperature threshold and changes relative to the past. Thus, areas showing no CSU in the past are excluded from the analysis. Due to the consideration of

Fig. 10 Same as Fig. 9, but for the far-future (2071–2095)
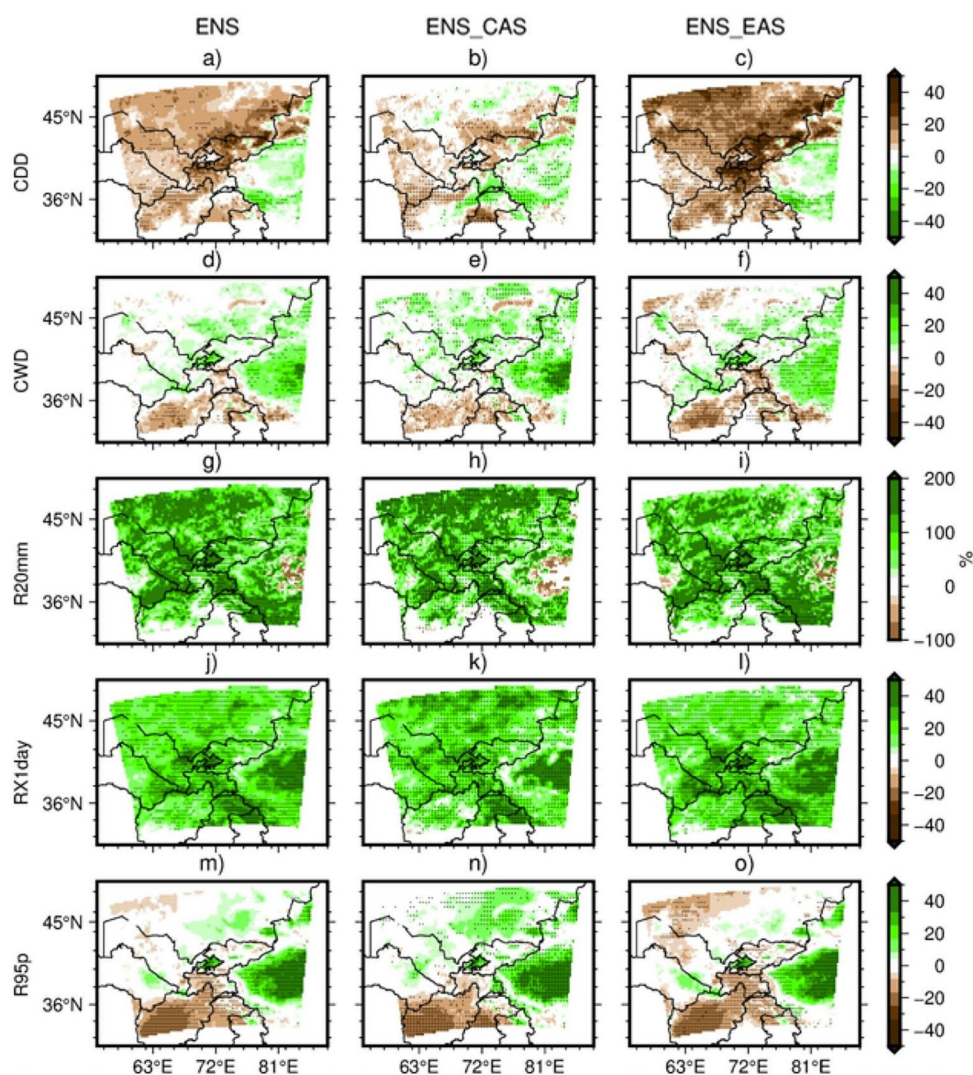
Fig. 11 Box and whisker plot for the projected change [%] in precipitation indices for the near- (2031–2055) and far-future (2071–2095) and all three ensembles (for corresponding absolute changes see Fig. S6)
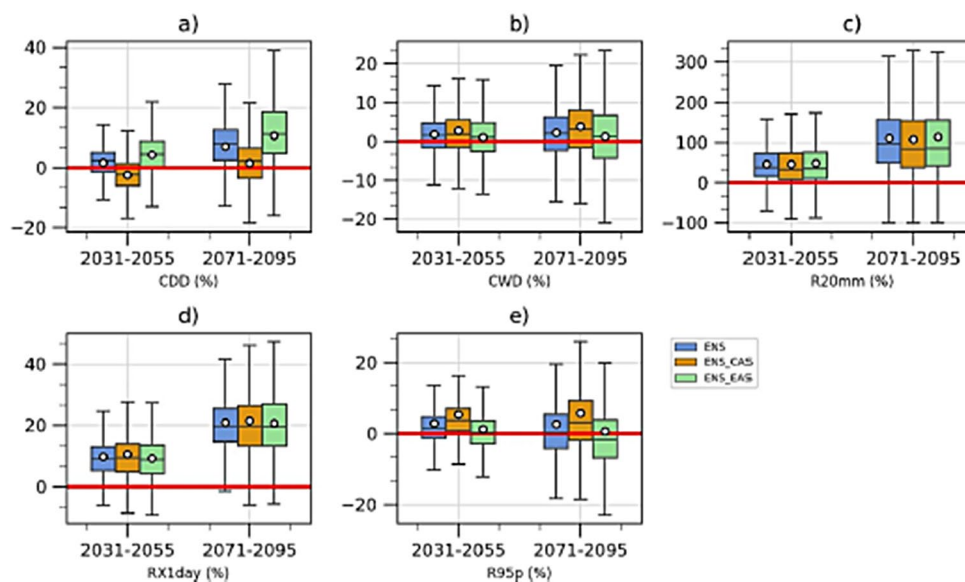
relative changes (absolute change values are shown in Fig. S8, and Fig. S9), the general increase of this index under RCP8.5 in all ensembles is strongest in the high mountain regions (Fig. 12a-c). The lowlands in the North and North-west show a moderate increase which is weaker in ENS_EAS (Fig. 12c). The immense rise of CSU in the lake areas of Aral and Balkhash can be related to the poor representation of temperatures by RCMs in these lake areas, as already mentioned in Sect. 3.1. Focusing on the far-future, CSU will further increase across much of the central and north-eastern parts (Fig. 13a-c). The projected changes are particularly stronger in the northernmost areas as depicted in ENS_CAS (Fig. 13b) while they are moderate for ENS and ENS_EAS (Fig. 13a and c).

CFD Considering CFDs, all three ensembles show a decrease in the near-future (Fig. 12d-f), with a further reduction expected at the end of the century (Fig. 13d-f). The patterns of change are comparably similar in the different ensembles with slightly less changes in desert and steppe areas of Xinjiang and Kazakhstan in ENS_EAS. Furthermore, the decrease will be smaller in orographic regions, such as Kyrgyzstan and Tajikistan, while the lowland areas of Kazakhstan, Uzbekistan, and Turkmenistan will experience a stronger shortening of CFD periods (Figs. 12d-f and 13d-f). Additionally, a dipole pattern can be observed in the eastern and western parts with comparatively stronger decrease in the western parts compared to the eastern parts.

HWDI The HWDI, a percentile-based index, is of utmost importance since heat waves are a major cause of weather-related fatalities. During the near-future, longer heat waves can be detected in all three ensembles over CEAS (Fig. 12g-i). However, the projections of HWDI during the middle of

the century in ENS_EAS are quite severe (> 800%), particularly over the orographic parts of the domain, in contrast to the changes shown by ENS_CAS (mostly < 400%, Fig. 12h and i). The smallest relative changes are observed over the lowland areas. By the end of the century, a more widespread and intensified HWDI is simulated in ENS_EAS (Fig. 13i) which is also the case for ENS_CAS, particularly in the southern and eastern parts of the domain, but with lower extent and shorter duration (Fig. 13h). Recently, Fallah et al. (2023) also found a higher risk of heat related extremes having a factor of four in the signal-to-noise-ratio over large parts of Central Asia.

TX10p and TX90p The two other percentile-based indices, TX10p and TX90p are calculated relative to the respective percentiles of the reference period. TX10p is projected to decrease during the near-future, with an almost similar spatial pattern across all three ensembles (Fig. 12j-l). However, the reduction is more pronounced over mountainous regions than in the plain areas across the ensembles (Fig. 12k and l). The decrease in the mountain areas is stronger in ENS_EAS than in ENS_CAS which is in line with the projected changes in CFD and HWDI. The magnitude of the simulated decrease is expected to amplify further at the end of the century (Fig. 13j-l).

In case of the percentage of very hot days, TX90p, the projected enhancement is predominantly spread across orographic and southern regions as shown by all three ensembles (Fig. 12m-o). The spatial patterns of TX90p are very similar to those of HWDI. By the end of the century, the more intense TX90p will extend over the entire study area (Fig. 13m-o). The regions south of Kyrgyzstan and Uzbekistan are especially affected by this development which can
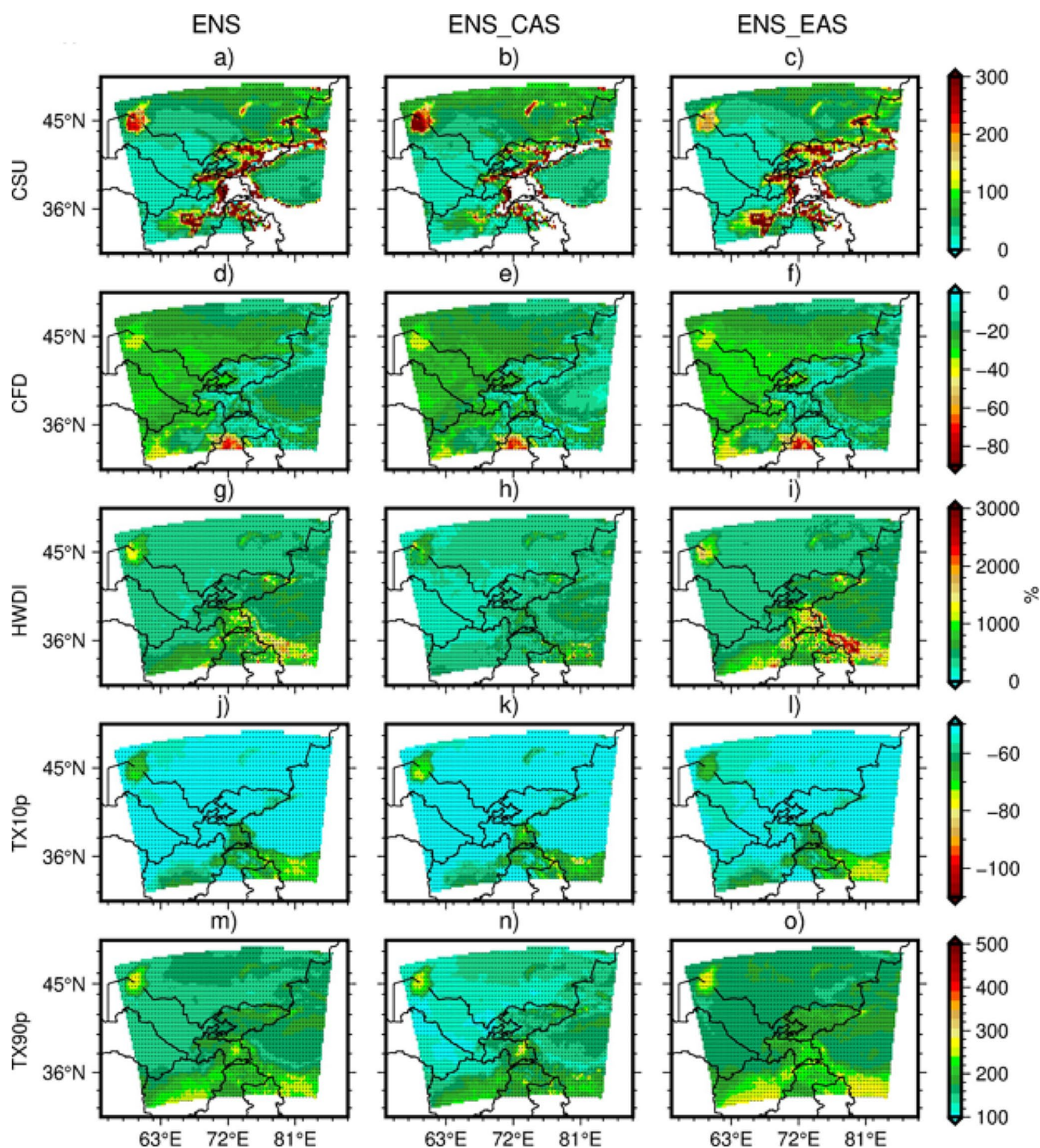
Fig. 12 Projected changes in temperature indices [%] from ENS (left column), ENS_CAS (center), and ENS_EAS (right) for the near-future (2031–2055) compared to the reference period (1981–2005). Stippling denotes grid points where more than 70% of the simulations agree on the sign of change

have an adverse effect on the energy demand, agricultural sector, and human health (Liu et al. 2020; Reyer et al. 2017).

Summary The spatial mean of the projected future changes in the temperature indices relative to the historical period is presented by a box and whisker plot in Fig. 14 (for corresponding absolute changes see Fig. S7). As mentioned

Fig. 13 Same as Fig. 12, but for the far-future (2071–2095)
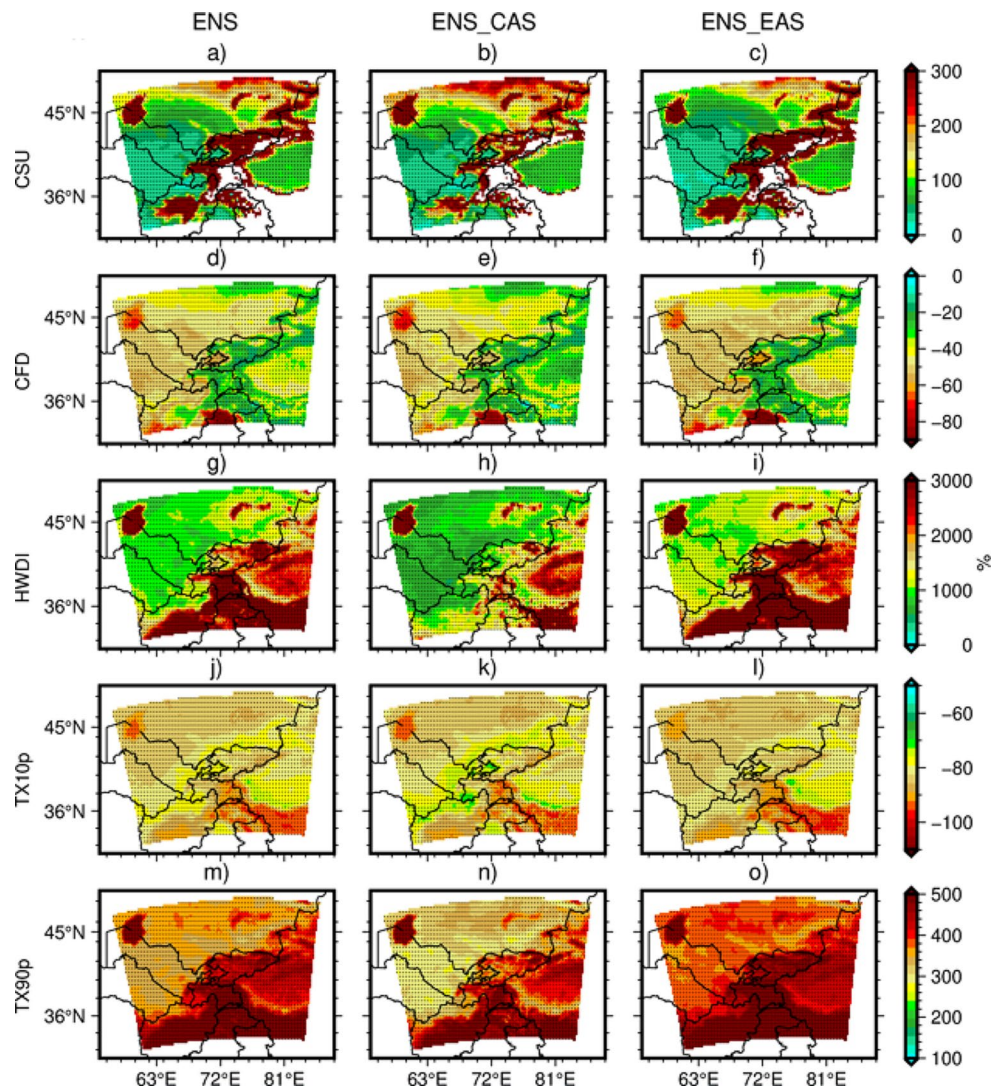
Fig. 14 Box and whisker plot for the projected change [%] in temperature indices for near- (2031–2055) and far-future (2071–2095) and all three ensembles (for corresponding absolute changes see Fig. S8)
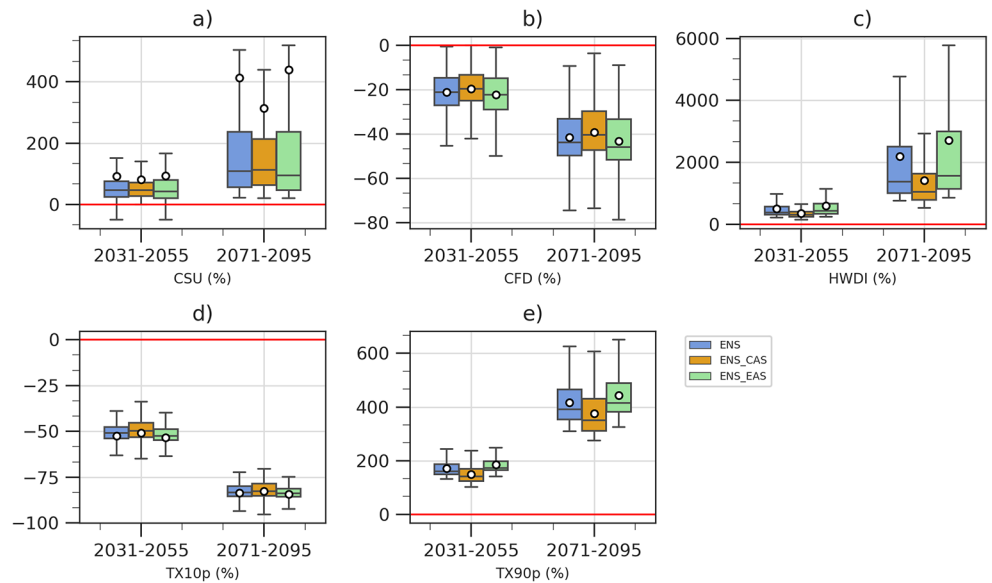
earlier, the ensembles from both ENS_CAS and ENS_EAS are aligned in the direction of change despite their varying magnitude of change depending on the considered variable. In comparison to the near-future, all three ensembles show a notable increase of consecutive summer days and a decrease of consecutive frost days in the far-future as shown in Fig. 14a and b. The relative amplification at the end of the century is strongest for extreme temperatures as demonstrated by HWDI (around 2000%) and TX90p (around 500%), with both trends being stronger in ENS_EAS than in ENS_CAS (Fig. 14c and e). Similar to the simulated decrease of CFD, the percentage of very cold days also tends to reduce substantially during the far-future (Fig. 14d). In summary, temperature related extremes are projected to either increase/decrease – depending on the index – in the future with further amplification at the end of the century. Thus, we expect a consistent pattern of warming and a decrease of cold extremes over time.

4 Discussion

The main incentive for using RCMs to provide future climate projections lies in their ability to provide higher spatial resolutions and better resolved land surface processes compared to GCMs, enabling a more accurate simulation of extreme events on local to regional scales (e.g., Coppola et al. 2021; Rummukainen 2016). However, the evaluation of RCMs is confronted with the issue of very few available high-resolution and high-quality meteorological datasets over Central Asia (e.g., Peña-Guerrero et al. 2022). Further, the station density of the region has been decreasing in the last decades which affects the quality of gridded products and makes model validation challenging (Hu et al. 2018). The gridded observation datasets, whose accuracy decreases with elevation (Peña-Guerrero et al. 2022; Zhu et al. 2015), generally underestimate solid precipitation (Sun et al. 2018). Indeed, RCMs show strong overestimations of precipitation in mountainous regions which is also the case in Central Asia (e.g., Rai et al. 2022; Top et al. 2021). The validation of RCMs becomes further challenging because gridded datasets tend to underestimate orographic precipitation (Zhu et al. 2015). A similar pattern of precipitation overestimation is also observed over orographic regions of our study domain in both ensembles (Fig. 3). The relatively good performance of ALARO-0 compared to REMO and RegCM might be caused by the application of different convection schemes together with a higher number of vertical layers where ALARO-0 has 47 (Top et al. 2021) while REMO and RegCM have 27 and 23, respectively (Giorgi et al. 2022). In the case of temperature, most of the

simulations show warm biases in the high-elevation parts of the domain, with the exception of ALARO-0, which displays a cold bias (Fig. 4). This behavior probably is related to deficiencies in ALARO-0's single-layer snow scheme (Top et al. 2021). The cold bias over the Tibetan Plateau and Himalayan region was also reported in the study of Russo et al. (2019) who attributed it to a reduced reliability of gridded validation products in these regions. A further systematic temperature bias of the RCMs is present in lake areas (Aral Sea, Lake Balkhash) where a strong warm bias persists. However, more advanced versions of the models than the ones provided by CORDEX-CORE are tackling this bias by coupling lake modules to the RCMs as it is done, for example, in REMO (Pietikäinen et al. 2018). Different signs of the minimum temperature bias at high elevations in the study of Rai et al. (2022) compared to Top et al. (2021) and our recent study might be attributed to different forcing data, time periods, validation data, model resolutions, or a combination of these effects.

Under RCP8.5, the projected changes in precipitation extremes show a general tendency towards more intense events. This is true for high precipitation amounts focusing on absolute precipitation values (R20mm, RX1day) in the entire domain, which is also shown by Zhu et al. (2020) who investigated simulations of the RCM WRF at 0.5° x 0.5° resolution. The percentile-based R95p shows a more dipole-like behavior with wetter conditions in the east and drier ones in the west. This is partly contradicting the study by Ozturk (2023) who examined simulations from RegCM4.3.5 - forced by two different GCMs and with a resolution of 50 km. The authors also found an increase of R95p by 20% over their domain, but the spatial patterns are not in line with the ones of Figs. 9 and 10 in our study. However, this could be caused by the smaller model ensemble, the usage of RegCM with its positive precipitation bias, the different reference period (1971–2000), and the coarser spatial resolution. The changes in the length of wet (CWD) and dry (CDD) periods depend on the region. Here, longer dry periods are detected in most areas with the exception of Xinjiang, while longer wet periods prevail in some mountainous parts of Kyrgyzstan and southern Kazakhstan. Additionally, stronger inter- or intra-seasonal variations are indicated for regions showing an increase of CWD and CDD. Regarding CDD, these findings are in line with Zhu et al. (2020). Other studies also reported a disagreement in projecting CDD using CMIP5 or CMIP6 simulations (Zhang and Wang 2022; Peng et al. 2020; Zhang and Zhou, 2020): the uncertainty among the models masks the change signal of CDD while the increase of other precipitation indices is robust and significant under global warming (Zhang and Wang 2022). The general increase of extreme precipitation events was also found in CMIP5

(Yao et al. 2021; Peng et al. 2020) and ISIMIP (Fallah et al. 2023) where the mountainous regions were revealed as being hotspots, too. Liu et al. (2020) identified a decrease of R95p with increased warming in Uzbekistan and Turkmenistan in CMIP6 leading to generally drier conditions which was also reported by Cao et al. (2023) and, for CMIP6, by Fallah et al. (2023) and Yao et al. (2021). Causes of these developments are the southward shift of the Subtropical Westerly Jet under future warming, leading to longer dry periods (Jiang and Zhou 2021), and, at the same time, the enhanced convergence of water vapor from the North Atlantic, West Pacific, and Arctic for extreme precipitation events shortly interrupting the dry periods (Wang et al. 2022). For Central Asia, the precipitation anomalies have been found to originate from a combination of changes in the westerly jet and in synoptic disturbances (Schiemann et al. 2008). Thus, large-scale circulation changes instead of changes of local moisture recycling are the driving force for hydrological changes in the region (Yao et al. 2021). Regarding the impacts, the increased number of CDDs goes along with enhanced droughts having significant effects on agriculture in the region (Qiu et al. 2023; Liu et al. 2020). Additionally, more heavy precipitation events are likely to increase the risk of landslides and mudflows, especially in the orographic regions of Kyrgyzstan and Tajikistan (Rakhmatullaev and Abdullaev 2014).

Central Asia, like many other parts of the world, has also experienced an increase of the duration, amplitude, and intensity of warm temperature extremes (Peng et al. 2020; Zhang et al. 2019c; Feng et al. 2018). In our study, the extreme temperature indices CSU, HWDI, and TX90p are projected to increase substantially over the entire region, while CFD and TX10p are projected to decrease. These described changes of temperature indices are supported by other studies using either RCMs (Ozturk 2023; Zhu et al. 2020) or GCMs (Fallah et al. 2023; Wu et al. 2023; Fan et al. 2022; Li et al. 2021; Peng et al. 2020). Ozturk (2023) and Zhu et al. (2020) also found CFD to decrease especially in mountain areas while the latter study also focused on CSU and identified the same patterns as revealed in our study. More frequent warm and heat events reduce the crop productivity and yield (Guglielmi 2022; Sutton et al. 2013) and result in an expansion of arid areas in Central Asia (Sorg et al. 2014). This goes along with decreased vegetation cover, changes in the hydrological cycle, and an increased irrigation water need for agriculture (Su et al. 2021; Luo et al. 2020). The latter plays a crucial role for food security but is difficult to assess by climate models since it depends on several additional prerequisites (Abel et al. 2024a): The issue becomes even more complex when water is not only provided by precipitation but also by snow and glacier melt.

Regarding the overlapping domain of the CAS and EAS ensembles we can conclude that the effect of the choice of the forcing GCM or the RCM is more prominent than the effect of the CORDEX-CORE domain. This is in line with the studies by Diez-Sierra et al. (2022b) and Legasa et al. (2020). However, Matte et al. (2017) found that differences arising from overlapping domains can be caused by an insufficient spin-up. Further, a proximity of the study region to the domain boundaries - which is the case in our study for ENS_EAS - can affect the model results of different domains in the overlapping area (Diez-Sierra et al. 2022b).

Differences between RCMs and GCMs over Central Asia can arise - beside different spatial resolutions - from different representations of seasonal snow cover as pointed out by Diez-Sierra et al. (2022b). Differences among the used RCMs can be attributed to different complexities of simulated processes and the usage of different parameterizations and underlying static surface data. Thus, Legasa et al. (2020) suggested enlarging the ensemble size of a domain by using additional GCM-RCM combinations from an overlapping domain. Even though the ensemble size is larger after inclusion of simulations from CORDEX-EAS, the interpretation of results must be done cautiously. Additionally, this does not necessarily help to overcome systematic biases like exemplified for the Aral Sea and Lake Balkhash. Furthermore, the need of higher resolved simulations is necessary as they are assumed to provide added value in complex mountain regions (Sangelantoni et al. 2023; Ban et al. 2021; Lucas-Picher et al. 2021). An alternative option is statistical downscaling when it comes to the correct representation of statistical distributions of local climate variables over complex orographic terrain (Benestad 2010).

On the impact side, the Central Asian population will directly be affected by the described changes of extreme events. For example, heat waves can affect the mortality among children, elderly people, and people working outside directly and through outbreaks of water- and vector-borne diseases (Reyer et al. 2017). Furthermore, aridity which is projected to increase further in the future over the Aral Sea basin, leads to frequent dust storms (Novikov et al. 2009), where exposure can cause respiratory diseases such as asthma (Griffin 2007). Higher temperatures result in glacial outburst flooding and mudflows which have already caused severe injuries and deaths in the region of Kyrgyzstan, Tajikistan, and Uzbekistan in the past (Novikov et al. 2009). Therefore, adaptation measures related to temperature and precipitation extremes are required, in the absence of which risks related to them will aggravate further.

5 Conclusion

Using a multi-model ensemble with ten members for an overlapping Central Asian domain (CEAS) from COR-DEX-CAS and CORDEX-EAS, projections of ten selected extreme indices related to precipitation and temperature are investigated in the present study. The selection of the over-lapping domain is motivated by a larger number of available ensemble members to achieve a more robust assessment of climate change signals and uncertainty ranges among the models. Note that the included models are not the same for both CORDEX domains. To account for the potential issues arising from this partly inconsistent ensemble we have analyzed all three ensembles (ENS, ENS_CAS, and ENS_EAS) regarding their projections of extreme events. In fact, we found the effect of the forcing data and the RCM to be more prominent than the domain effect.

Focusing on daily precipitation and temperature, ALARO-0 and REMO are generally outperforming RegCM. However, there is also a strong dependency on the driving GCM as it is demonstrated by the warm bias introduced by NorESM1-M-forcing. Furthermore, all RCMs underlie sig-nificant temperature biases in lake areas. During the histori-cal period, the extreme indices are represented best by the ensemble mean over all simulations with a generally better performance of ENS_CAS compared to ENS_EAS. This is due to the presence of systematic and wide-spread tempera-ture and precipitation biases of RegCM that is part of the ENS_EAS ensemble.

For the future we can state that extreme precipitation events will increase especially in mountain areas although the spatial patterns vary among the sub-ensembles. The changes in CDD and CWD depend on the models as well, but longer dry periods clearly prevail in the southern part of the study area. Regions showing an increase of CDD (+7.8% / +5.6 days) and CWD (+2.09% / +0.08 days) tend to experience a more intense inter- or intra-seasonal vari-ability in the future. Temperature indices referring to warm and dry events, e.g., CSU (+108.5% / +38.3 days), HWDI (+1379.1% / +91.37 days), and TX90p (+391.1% / +34.54 days), show a persistent intensification, while the occur-rence of cold events, e.g., CFD (-43.7% / -25.2 days), and TX10p (-83.4% / -8.13 days), reduces systematically. The changes are most prominent at higher-elevation sites which is partly due to the considered relative instead of absolute changes. All patterns show a further intensification from the near- to the far-future and, thus, for ongoing greenhouse gas emissions and global warming.

The complex topography of the area poses various chal-lenges. This is true for available gridded validation data as well as the model simulations, as both show a reduced qual-ity in such regions. Thus, the availability of further in-situ

stations and more RCM simulations with improved land-surface processes, e.g., with respect to snow cover, land use, lake effects and soil hydrology, and higher resolutions are necessary to reduce the uncertainties of the projected changes in climate and weather extremes, as presented in this study. Independent of that, it is necessary to mitigate and adapt to future changes in the examined extreme indi-ces as they can have tremendous effects on heat, drought, and floods and, in consequence, on water and energy supply, agriculture, food security, and aspects of human health. Fur-ther research is needed to reduce the mentioned uncertain-ties and tackle the impacts of climate change. Additionally, a seasonal focus of the model representation as done, e.g., by Rai et al. (2022) or Zhu et al. (2020), will be reasonable due to the strong seasonality of Central Asia's climate.

Declarations

Competing interests The authors declare no competing interests.

References

Abel DKJ (2023) Weiterentwicklung der Bodenhydrologie des regionalen Klimamodells REMO (Doctoral dissertation, Universität Würzburg). https://doi.org/10.25972/OPUS-31146

Abel D, Ziegler K, Gbode IE, Weber T, Ajayi VO, Traoré SB et al (2024a) Robustness of climate indices relevant for agriculture in Africa deduced from GCMs and RCMs against reanalysis and gridded observations. Clim Dyn 62:1077–1106. https://doi.org/10.1007/s00382-023-06956-8

Abel D, Ziegler K, Apel H, Huth J, Nguyen DV, Tguyen HV et al (2024b) Intercomparison of gridded precipitation products in Vietnam and Mainland Southeast Asia. International Journal of Climatology, in Review

Ballester J, Quijal-Zamorano M, Méndez Turrubiates RF, Pegenaute F, Herrmann FR, Robine JM et al (2023) Heat-related mortality in Europe during the summer of 2022. Nat Med 29:1857–1866. https://doi.org/10.1038/s41591-023-02419-z

Ban N, Caillaud C, Coppola E, Pichelli E, Sobolowski S, Adinolfi M et al (2021) The first multi-model ensemble of regional climate simulations at kilometer-scale resolution, part I: evaluation of precipitation. Clim Dyn 57:275–302. https://doi.org/10.1007/s00382-021-05708-w

Bangelesa F, Abel D, Pollinger F, Rai P, Ziegler K, Ebengo D et al (2023) Projected changes in rainfall amount and distribution in the Democratic Republic of Congo – evidence from an ensemble of high-resolution climate simulations. Weather Clim Extremes 42:100620. https://doi.org/10.1016/j.wace.2023.100620

Barlow MA, Tippett MK (2008) Variability and predictability of central Asia river flows: antecedent winter precipitation and large-scale teleconnections. J Hydrometeorol 9(6):1334–1349. https://doi.org/10.1175/2008JHM976.1

Beck HE, Van Dijk AI, Levizzani V, Schellekens J, Miralles DG, Martens B, De Roo A (2017a) MSWEP: 3-hourly 0.25_ global gridded precipitation (1979–2015) by merging gauge, satellite, and reanalysis data. Hydrol Earth Syst Sci 21(1):589–615. https://doi.org/10.5194/hess-21-589-2017

Beck HE, Vergopolan N, Pan M, Levizzani V, Van Dijk AI, Weedon GP et al (2017b) Global-scale evaluation of 22 precipitation datasets using gauge observations and hydrological modeling. Hydrol Earth Syst Sci 21(12):6201–6217. https://doi.org/10.5194/hess-21-6201-2017

Beck HE, Wood EF, Pan M, Fisher CK, Miralles DG, Van Dijk AIJM et al (2019) MSWEP V2 global 3-hourly 0.1_ precipitation: methodology and quantitative assessment. Bull Am Meteorol Soc 100(3):473–500. https://doi.org/10.1175/BAMS-D-17-0138.1

Beck HE, Wood EF, Pan M, Fisher CK, Miralles DG, van Dijk AIJM et al (2021) MSWEP V2.8 technical documentation. http://www.gloh2o.org/mswep/

Benestad RE (2010) Downscaling precipitation extremes: correction of analog models through PDF predictions. Theoret Appl Climatol 100:1–21. https://doi.org/10.1007/s00704-009-0158-1

Boussetta S, Balsamo G, Beljaars A, Panareda AA, Calvet JC, Jacobs C et al (2013) Natural land carbon dioxide exchanges in the ECMWF Integrated forecasting system: implementation and offline validation. J Geophys Research: Atmos 118(12):5923–5946. https://doi.org/10.1002/jgrd.50488

Cao L, Xu C, Suo N, Song L, Lei X (2023) Future dry-wet climatic characteristics and drought trends over arid central Asia. Front Earth Sci 11:1102633. https://doi.org/10.3389/feart.2023.1102633

Chen F, Huang W, Jin L, Chen J, Wang J (2011) Spatiotemporal precipitation variations in the arid Central Asia in the context of global warming. Sci China Earth Sci 54:1812–1821. https://doi.org/10.1007/s11430-011-4333-8

Chevallier P, Pouyaud B, Mojaïsky M, Bolgov M, Olsson O, Bauer M, Froebrich J (2014) River flow regime and snow cover of the Pamir Alay (Central Asia) in a changing climate. Hydrol Sci J 59(8):1491–1506. https://doi.org/10.1080/02626667.2013.838004

Coppola E, Raffaele F, Giorgi F, Giuliani G, Xuejie G, Ciarlo JM et al (2021) Climate hazard indices projections based on CORDEX-CORE, CMIP5 and CMIP6 ensemble. Clim Dyn 57:1293–1383. https://doi.org/10.1007/s00382-021-05640-z

D'Ippoliti D, Michelozzi P, Marino C, de'Donato F, Menne B, Katsouyanni K et al (2010) The impact of heat waves on mortality in 9 European cities: results from the EuroHEAT project. Environ Health 9(1):37–37. https://doi.org/10.1186/1476-069X-9-37

Das J, Umamahesh NV (2022) Heat wave magnitude over India under changing climate: projections from CMIP5 and CMIP6 experiments. Int J Climatol 42(1):331–351. https://doi.org/10.1002/joc.7246

Diez-Sierra J, Iturbide M, Gutiérrez JM, Fernández J, Milovac J, Cofiño AS et al (2022a) CORDEX model component description. Zenodo. https://doi.org/10.5281/zenodo.6553526

Diez-Sierra J, Iturbide M, Gutiérrez JM, Fernández J, Milovac J, Cofiño AS et al (2022b) The worldwide C3S CORDEX grand ensemble: a major contribution to assess regional climate change in the IPCC AR6 Atlas. Bull Am Meteorol Soc 103(12):E2804–E2826. https://doi.org/10.1175/BAMS-D-22-0111.1

Dike VN, Lin Z, Fei K, Langendijk GS, Nath D (2022) Evaluation and multi model projection of seasonal precipitation extremes over central Asia based onCMIP6 simulations. Int J Climatol 42(14):7228–7251. https://doi.org/10.1002/joc.7641

Fallah B, Russo E, Menz C, Hoffmann P, Didovets I, Hattermann FF (2023) Anthropogenic influence on extreme temperature and precipitation in Central Asia. Sci Rep 13(1):6854. https://doi.org/10.1038/s41598-023-33921-6

Fan LJ, Yan ZW, Chen D, Li Z (2022) Assessment of central Asian heat extremes by statistical downscaling: validation and future projection for 2015–2100. Adv Clim Change Res 13(1):14–27. https://doi.org/10.1016/j.accre.2021.09.007

Feng R, Yu R, Zheng H, Gan M (2018) Spatial and temporal variations in extreme temperature in Central Asia. Int J Climatol 38:e388–e400. https://doi.org/10.1002/joc.5379

Fischer EM, Knutti R (2015) Anthropogenic contribution to global occurrence of heavy-precipitation and high-temperature extremes. Nat Clim Change 5(6):560–564. https://doi.org/10.1038/nclimate2617

Gao X, Shi Y, Han Z, Wang M, Wu J, Zhang D et al (2017) Performance of RegCM4 over major river basins in China. Adv Atmos Sci 34:441–455. https://doi.org/10.1007/s00376-016-6179-7

Gibba P, Sylla MB, Okogbue EC, Gaye AT, Nikiema M, Kebe I (2019) State-of-the-art climate modeling of extreme precipitation over Africa: analysis of CORDEX added-value over CMIP5. Theoret Appl Climatol 137:1041–1057. https://doi.org/10.1007/s00704-018-2650-y

Giorgi F, Jones C, Asrar GR (2009) Addressing climate information needs at the regional level: the CORDEX framework. World Meteorological Organ (WMO) Bull 58(3):175

Giorgi F, Coppola E, Solmon F, Mariotti L, Sylla MB, Bi X et al (2012) RegCM4: model description and preliminary tests over multiple CORDEX domains. Climate Res 52:7–29. https://doi.org/10.3354/cr01018

Giorgi F, Coppola E, Jacob D, Teichmann C, Abba Omar S, Ashfaq M et al (2022) The CORDEX-CORE EXP-I initiative: description and highlight results from the initial analysis. Bull Am Meteorol Soc 103(2):E293–E310. https://doi.org/10.1175/BAMS-D-21-0119.1

Griffin DW (2007) Atmospheric movement of microorganisms in clouds of desert dust and implications for human health. Clin Microbiol Rev 20(3):459–477. https://doi.org/10.1128/cmr.00039-06

Gu H, Yu Z, Peltier WR et al (2020) Sensitivity studies and comprehensive evaluation of RegCM4.6.1 high-resolution climate simulations over the Tibetan Plateau. Clim Dyn 54:3781–3801. https://doi.org/10.1007/s00382-020-05205-6

Guglielmi G (2022) Climate change is turning more of Central Asia into desert. Nature. https://doi.org/10.1038/d41586-022-01667-2

Guo H, Bao A, Chen T, Zheng G, Wang Y, Jiang L, De Maeyer P (2021) Assessment of CMIP6 in simulating precipitation over arid Central Asia. Atmos Res 252:105451. https://doi.org/10.1016/j.atmosres.2021.105451

Gutowski WJ Jr, Giorgi F, Timbal B, Frigon A, Jacob D, Kang HS et al (2016) WCRP COordinated Regional Downscaling EXperiment (CORDEX): a diagnostic MIP for CMIP6. Geosci Model Dev 9(11):4087–4095. https://doi.org/10.5194/gmd-9-4087-2016

Hu Z, Li Q, Chen X, Teng Z, Chen C, Yin G, Zhang Y (2016) Climate changes in temperature and precipitation extremes in an alpine grassland of Central Asia. Theoretical Appl Climatology 126(3–4):519–531. https://doi.org/10.1007/s00704-015-1568-x

Hu Z, Zhou Q, Chen X, Li J, Li Q, Chen D et al (2018) Evaluation of three global gridded precipitation data sets in central Asia based on rain gauge observations. Int J Climatol 38(9):3475–3493. https://doi.org/10.1002/joc.5510

Huang J, Yu H, Guan X, Wang G, Guo R (2015) Accelerated dryland expansion under climate change. Nat Clim Change 6(2):166–171. https://doi.org/10.1038/nclimate2837

IPCC (2021) Climate change 2021: the physical science basis [M/OL]. https://www.ipcc.ch/report/ar6/wg1/downloads/report/IPCC_AR6_WGI_Full_Report.pdf (Accessed on: 01.08.21)

Jacob D, Elizalde A, Haensler A, Hagemann S, Kumar P, Podzun R et al (2012) Assessing the transferability of the regional climate model REMO to different coordinated regional climate downscaling experiment (CORDEX) regions. Atmosphere 3(1):181–199. https://doi.org/10.3390/atmos3010181

Jacob D, Kotova L, Teichmann C, Sobolowski SP, Vautard R, Donnelly C et al (2018) Climate impacts in Europe under +1.5°C global warming. Earth's Future 6(2):264–285. https://doi.org/10.1002/2017EF000710

Jacob D, Teichmann C, Sobolowski S, Katragkou E, Anders I, Belda M et al (2020) Regional climate downscaling over Europe: perspectives from the EURO-CORDEX community. Reg Envriron Chang 20:1–20. https://doi.org/10.1007/s10113-020-01606-9

Jiang J, Zhou T (2021) Human-induced rainfall reduction in drought-prone northern Central Asia. Geophys Res Letter 48(7). https://doi.org/10.1029/2020GL092156. e2020GL092156

John A, Douville H, Ribes A, Yiou P (2022) Quantifying CMIP6 model uncertainties in extreme precipitation projections. Weather Clim Extremes 36:100435. https://doi.org/10.1016/j.wace.2022.100435

Kenzhebaev R, Barandun M, Kronenberg M, Chen Y, Usubaliev R, Hoelzle M (2017) Mass balance observations and reconstruction for Batysh Sook Glacier, Tien Shan, from 2004 to 2016. Cold Reg Sci Technol 135:76–89. https://doi.org/10.1016/j.coldregions.2016.12.007

Kim YH, Min SK, Zhang X, Sillmann J, Sandstad M (2020) Evaluation of the CMIP6 multi-model ensemble for climate extreme indices. Weather Clim Extremes 29:100269. https://doi.org/10.1016/j.wace.2020.100269

Kraaijenbrink PD, Stigter EE, Yao T, Immerzeel WW (2021) Climate change decisive for Asia's snow meltwater supply. Nat Clim Change 11(7):591–597. https://doi.org/10.1038/s41558-021-01074-x

Legasa MN, Manzanas R, Fernández J, Herrera S, Iturbide M, Moufouma-Okia W et al (2020) Assessing multidomain overlaps and grand ensemble generation in CORDEX regional projections. Geophys Res Lett 47(4). https://doi.org/10.1029/2019GL086799. e2019GL086799

Li C, Zwiers F, Zhang X, Li G, Sun Y, Wehner M (2021) Changes in annual extremes of daily temperature and precipitation in CMIP6 models. J Clim 34(9):3441–3460. https://doi.org/10.1175/JCLI-D-19-1013.1

Li LL, Cao J, Yu RC (2022a) Evaluation of CMIP6 HighResMIP models in simulating precipitation over Central Asia. Adv Clim Change Res 13:1–13. https://doi.org/10.1016/j.accre.2021.09.009

Li M, Lv X, Zhu L, Uchenna Ochege F, Guo H (2022b) Evaluation and application of MSWEP in Drought Monitoring in Central Asia. Atmosphere 13:1053. https://doi.org/10.3390/atmos13071053

Lindvall J, Svensson G (2015) The diurnal temperature range in the CMIP5 models. Climate Dyn., 44, 405–421. https://doi.org/10.1007/s00382-014-2144-2.

Liu Y, Geng X, Hao Z, Zheng J (2020) Changes in climate extremes in Central Asia under 1.5 and 2 C global warming and their impacts on agricultural productions. Atmosphere 11(10):1076. https://doi.org/10.3390/atmos11101076

Liu Z, Huang J, Xiao X, Tong X (2022) The capability of CMIP6 models on seasonal precipitation extremes over Central Asia. Atmos Res 278:106364. https://doi.org/10.1016/j.atmosres.2022.106364

Lucas-Picher P, Argüeso D, Brisson E, Tramblay Y, Berg P, Lemonsu A et al (2021) Convection-permitting modeling with regional climate models: latest developments and next steps. WIREs Clim Change 12(6):e731. https://doi.org/10.1002/wcc.731

Luo M, Sa C, Meng F, Duan Y, Liu T, Bao Y (2020) Assessing extreme climatic changes on a monthly scale and their implications for vegetation in Central Asia. J Clean Prod 271:122396. https://doi.org/10.1016/j.jclepro.2020.122396

Maharana P, Kumar D, Das S, Tiwari PR (2021) Present and future changes in precipitation characteristics during Indian summer monsoon in CORDEX-CORE simulations. Int J Climatol 41(3):2137–2153. https://doi.org/10.1002/joc.6951

Mannig B, Müller M, Starke E, Merkenschlager C, Mao W, Zhi X et al (2013) Dynamical downscaling of climate change in Central Asia. Global Planet Change 110:26–39. https://doi.org/10.1016/j.gloplacha.2013.05.008

Mannig B, Pollinger F, Gafurov A, Vorogushyn S, Unger-Shayesteh K (2018) Impacts of climate change in Central Asia. Encyclopedia Anthropocene 195–203. https://doi.org/10.1016/B978-0-12-809665-9.09751-2. Elsevier

Mašek J (2017) Problem with screen level temperatures above snow in ISBA scheme, report RC LACE. https://www.rclace.eu/File/Physics/2017/masek_isba_snow2_Mar2017.pdf (Accessed on: 07.07.23)

Matte D, Laprise R, Thériault JM, Lucas-Picher P (2017) Spatial spin-up of fine scales in a regional climate model simulation driven by low-resolution boundary conditions. Clim Dyn 49:563–574. https://doi.org/10.1007/s00382-016-3358-2

Meier C, Knoche M, Merz R, Weise SM (2013) Stable isotopes in river waters in the Tajik pamirs: regional and temporal characteristics. Isot Environ Health Stud 49(4):542–554. https://doi.org/10.1080/10256016.2013.835809

Moss RH, Edmonds JA, Hibbard KA, Manning MR, Rose SK, Van Vuuren DP et al (2010) The next generation of scenarios for climate change research and assessment. Nature 463(7282):747–756. https://doi.org/10.1038/nature08823

Muñoz-Sabater J, Dutra E, Agustí-Panareda A, Albergel C, Arduini G, Balsamo G et al (2021) Earth Syst Sci Data 13(9):4349–4383. https://doi.org/10.5194/essd-13-4349-2021. ERA5-Land: a state-of-the-art global reanalysis dataset for land applications

Nanditha JS, Kushwaha AP, Singh R, Malik I, Vegad U, Dangar S et al (2023) The Pakistan Flood of August 2022: causes and implications. Earth's Future 11(3). https://doi.org/10.1029/2022EF003230. e2022EF003230

Novikov V, Simonett O, Beilstein M, Bournay E, Berthiaume C, Kirby A, Rajabov I (2009) Climate change in Central Asia—a visual synthesis. Swiss Federal Office for the environment (FOEN). Zoï Environment Network

Oh SG, Park JH, Lee SH et al (2014) Assessment of the RegCM4 over East Asia and future precipitation change adapted to the RCP scenarios. J Geophys Research: Atmos 119:2913–2927. https://doi.org/10.1002/2013JD020693

Ozturk T (2023) Projected future changes in Extreme Climate indices over Central Asia using RegCM4.3.5. Atmosphere 14(6):939. https://doi.org/10.3390/atmos14060939

Ozturk T, Altinsoy H, Türkeş M, Kurnaz ML (2012) Simulation of temperature and precipitation climatology for the Central Asia CORDEX domain using RegCM 4.0. Climate Res 52:63–76. https://doi.org/10.3354/cr01082

Ozturk T, Turp MT, Türkeş M, Kurnaz ML (2017) Projected changes in temperature and precipitation climatology of Central Asia CORDEX Region 8 by using RegCM4.3.5. Atmos Res 183:296–307. https://doi.org/10.1016/j.atmosres.2016.09.008

Paeth H, Schönbein D, Keupp L, Abel D, Bangelesa F, Baumann M et al (2023) Climate change information tailored to the agricultural sector in Central Europe, exemplified on the region of Lower Franconia. Clim Change 176(10):136. https://doi.org/10.1007/s10584-023-03613-1

Park JH, Oh SG, Suh MS (2013) Impacts of boundary conditions on the precipitation simulation of RegCM4 in the CORDEX East Asia domain. J Geophys Research: Atmos 118:1652–1667. https://doi.org/10.1002/jgrd.5019

Peña-Guerrero MD, Umirbekov A, Tarasova L, Müller D (2022) Comparing the performance of high-resolution global precipitation products across topographic and climatic gradients of Central Asia. Int J Climatol 42(11):5554–5569. https://doi.org/10.1002/joc.7548

Peng D, Zhou T, Zhang L, Zhang W, Chen X (2020) Observationally constrained projection of the reduced intensification of extreme climate events in Central Asia from 0.5°C less global warming. Clim Dyn 54:543–560. https://doi.org/10.1007/s00382-019-05014-6

Pietikäinen JP, Markkanen T, Sieck K, Jacob D, Korhonen J, Räisänen P et al (2018) The regional climate model REMO (v2015) coupled with the 1-D freshwater lake model FLake (v1): Fenno-Scandinavian climate and lakes. Geosci Model Dev 11(4):1321–1342. https://doi.org/10.5194/gmd-11-1321-2018

Prein AF, Gobiet A (2017) Impacts of uncertainties in European gridded precipitation observations on regional climate analysis. Int J Climatol 37(1):305. https://doi.org/10.1002/joc.4706

Pritchard HD (2017) Asia's glaciers are 705 a regionally important buffer against drought. Nature 545(7653):169–174. https://doi.org/10.1038/nature22062

Qiu Y, Yan Z, Feng J, Hua L, Fan L, Li Z et al (2023) Robust historical and future drying trends in Central Asia evidenced by the latest observation and modeling datasets. Atmos Res 107033. https://doi.org/10.1016/j.atmosres.2023.107033

Rai P, Choudhary A, Dimri AP (2019) Future precipitation extremes over India from the CORDEX-South Asia experiments. Theoret Appl Climatol 137(3–4):2961–2975. https://doi.org/10.1007/s00704-019-02784-1

Rai P, Ziegler K, Abel D, Pollinger F, Paeth H (2022) Performance of a regional climate model with interactive vegetation (REMO-iMOVE) over Central Asia. Theoret Appl Climatol 150(3–4):1385–1405. https://doi.org/10.1007/s00704-022-04233-y

Rai P, Abel D, Ziegler K, Pollinger F, Paeth H (2023) Effect of an irrigation scheme implemented in a regional climate model over Central Asia. EGU General Assembly 2023, Vienna, Austria, 24–28 Apr 2023, EGU23-16125 https://doi.org/10.5194/egusphere-egu23-16125

Rakhmatullaev S, Abdullaev I (2014) Central Asian irrigation sector in a climate change context: some reflections. J Water Clim Change 5(3):341–356. https://doi.org/10.2166/wcc.2014.120

Reboita MS, da Rocha RP, Souza CAD, Baldoni TC, Silva PLLDS, Ferreira GWS (2022) Future projections of Extreme Precipitation Climate indices over South America based on CORDEX-CORE Multimodel Ensemble. Atmosphere 13(9):1463. https://doi.org/10.3390/atmos13091463

Remedio AR, Teichmann C, Buntemeyer L, Sieck K, Weber T, Rechid D et al (2019) Evaluation of New CORDEX simulations using an updated Köppen–Trewartha climate classification. Atmosphere 10(11):726. https://doi.org/10.3390/atmos10110726

Reyer CP, Otto IM, Adams S, Albrecht T, Baarsch F, Cartsburg M et al (2017) Climate change impacts in Central Asia and their implications for development. Reg Envriron Chang 17(6):1639–1650. https://doi.org/10.1007/s10113-015-0893-z

Robinson A, Lehmann J, Barriopedro D, Rahmstorf S, Coumou D (2021) Increasing heat and rainfall extremes now far outside the historical climate. Npj Clim Atmospheric Sci 4(1):45. https://doi.org/10.1038/s41612-021-00202-w

Rummukainen M (2010) State-of-the-art with regional climate models. Wiley Interdisciplinary Reviews: Clim Change 1(1):82–96. https://doi.org/10.1002/wcc.8

Rummukainen M (2016) Added value in regional climate modeling. Wiley Interdisciplinary Review: Clim Change 7(1):145–159. https://doi.org/10.1002/wcc.378

Russo E, Kirchner I, Pfahl S, Schaap M, Cubasch U (2019) Sensitivity studies with the regional climate model COSMO-CLM 5.0 over the CORDEX Central Asia Domain. Geosci Model Dev 12:5229–5249. https://doi.org/10.5194/gmd-12-5229-2019

Samuel S, Dosio A, Mphale K, Faka DN, Wiston M (2023) Comparison of multimodel ensembles of global and regional climate models projections for extreme precipitation over four major river basins in southern Africa—assessment of the historical simulations. Clim Change 176(5):57. https://doi.org/10.1007/s10584-023-03530-3

Sangelantoni L, Sobolowski S, Lorenz T, Hodnebrog Ø, Cardoso RM, Soares PMM et al (2023) Investigating the representation of heatwaves from an ensemble of km-scale regional climate simulations within CORDEX-FPS convection. https://doi.org/10.1007/s00382-023-06769-9. Climate Dynamics

Schiemann R, Lüthi D, Vidale PL, Schär C (2008) The precipitation climate of Central Asia—Intercomparison of observational and numerical data sources in a remote semiarid region. Int J Climatol 28(3):295–314. https://doi.org/10.1002/joc.1532

Schulzweida U (2019) CDO User Guide. https://code.zmaw.de/projects,cdo/embedded/cdo.pdf

Seddon AW, Macias-Fauria M, Long PR, Benz D, Willis KJ (2016) Sensitivity of global terrestrial ecosystems to climate variability. Nature 531(7593):229–232. https://doi.org/10.1038/nature16986

Sobie SR, Zwiers FW, Curry CL (2021) Climate model projections for Canada: a comparison of CMIP5 and CMIP6. Atmos Ocean

59(4–5):269–284. https://doi.org/10.1080/07055900.2021.2011103

Sorg A, Huss M, Rohrer M, Stoffel M (2014) The days of plenty might soon be over in glacierized central Asian catchments. Environ Res Lett 9(10):104018. https://doi.org/10.1088/1748-9326/9/10/104018

Spinoni J, Barbosa P, Bucchignani E, Cassano J, Cavazos T, Christensen JH et al (2020) Future global meteorological drought hotspots: a study based on CORDEX data. J Clim 33(9):3635–36561. https://doi.org/10.1175/JCLI-D-19-0084.1

Spinoni J, Barbosa P, Bucchignani E, Cassano J, Cavazos T, Cescatti A et al (2021) Global exposure of population and land-use to meteorological droughts under different warming levels and SSPs: a CORDEX-based study. Int J Climatol 41(15):6825–6853. https://doi.org/10.1002/joc.7302

Su Y, Li Y, Liu Y, Huang G, Jia Q, Li Y (2021) An integrated multi-GCMs bayesian-neural-network hydrological analysis method for quantifying climate change impact on runoff of the Amu Darya River basin. Int J Climatol 41(5):3411–3424. https://doi.org/10.1002/joc.7026

Sun Q, Miao C, Duan Q, Ashouri H, Sorooshian S, Hsu KL (2018) Rev Geophys 56(1):79–107. https://doi.org/10.1002/2017RG000574. A review of global precipitation data sets: data sources, estimation, and inter-comparisons

Sutton WR, Srivastava JP, Neumann JE, Iglesias A, Boehlert BB (2013) Reducing the vulnerability of Uzbekistan's Agricultural systems to Climate Change. Impact Assessment and Adaptation options. World Bank Study. https://doi.org/10.1596/978-1-4648-0000-9. Washington, DC

Teichmann C, Jacob D, Remedio AR, Remke T, Buntemeyer L, Hoffmann P et al (2021) Assessing mean climate change signals in the global CORDEX-CORE ensemble. Clim Dyn 57:1269–1292. https://doi.org/10.1007/s00382-020-05494-x

Termonia P, Fischer C, Bazile E, Bouyssel F, Brožková R, Bénard P, Bochenek B, Degrauwe D, Derková M, El Khatib R, Hamdi R, Mašek J, Pottier P, Pristov N, Seity Y, Smolíková P, Španiel O, Tudor M, Wang Y, Wittmann C, Joly A (2018) The ALADIN System and its canonical model configurations AROME CY41T1 and ALARO CY40T1, Geosci. Model Dev 11:257–281. https://doi.org/10.5194/gmd-11-257-2018

Top S, Kotova L, De Cruz L, Aniskevich S, Bobylev L, De Troch R et al (2021) Evaluation of regional climate models ALARO-0 and REMO2015 at 0.22 resolution over the CORDEX Central Asia domain. Geosci Model Dev 14(3):1267–1293. https://doi.org/10.5194/gmd-14-1267-2021

Uieda L, Tian D, Leong WJ, Toney L, Schlitzer W, Yao J et al (2021) PyGMT: a Python interface for the generic mapping tools [Software]. https://doi.org/10.5281/zenodo.4592991. Zenodo

Van Loon AF, Tijdeman E, Wanders N, Van Lanen HJ, Teuling AJ, Uijlenhoet R (2014) How climate seasonality modifies drought duration and deficit. J Geophys Research: Atmos 119(8):4640–4656. https://doi.org/10.1002/2013JD020383

Van Vuuren DP, Edmonds J, Kainuma M, Riahi K, Thomson A, Hibbard K et al (2011) The representative concentration pathways: an overview. Clim Change 109:5–31. https://doi.org/10.1007/s10584-011-0148-z

Wang K, Clow GD (2020) The diurnal temperature range in CMIP6 models: Climatology, variability, and evolution. Journal of Climate, 33(19), 8261–8279. https://doi.org/10.1175/jcli-d-19-0897.1

Wang H, Zhang J, Chen L, Li D (2022) Relationship between summer extreme precipitation anomaly in Central Asia and surface sensible heat variation on the central-eastern Tibetan plateau. Clim Dyn 59(3–4):685–700. https://doi.org/10.1007/s00382-022-06148-w

Waskom ML (2021) Seaborn: statistical data visualization. J Open Source Softw 6(60):3021. https://doi.org/10.21105/joss.03021

Wessel P, Luis JF, Uieda L, Scharroo R, Wobbe F, Smith WHF, Tian D (2019a) The generic mapping tools version 6 [Software]. Zenodo. (Funded by US National Science Foundation grants OCE-1558403 and EAR-1829371). https://doi.org/10.5281/zenodo.3407866

Wessel P, Luis JF, Uieda L, Scharroo R, Wobbe F, Smith WHF, Tian D (2019b) The generic mapping tools version 6. Geochem Geophys Geosyst 20(11):5556–5564. https://doi.org/10.1029/2019gc008515

World Bank (2012) Turn down the heat: why a 4°C warmer world must be avoided. World Bank, Washington DC. http://documents.worldbank.org/curated/en/865571468149107611/Turn-down-the-heat-why-a-4-C-warmer-world-must-be-avoided

Wu L, Zhao C, Li J, Yan Y, Han Q, Li C, Zhu J (2023) Impact of extreme climates on land surface phenology in Central Asia. Ecol Ind 146:109832. https://doi.org/10.1016/j.ecolind.2022.109832

Xu W, Lei X, Chen S, Yu T, Hu Z, Zhang M et al (2022) How well does the ERA5 reanalysis capture the Extreme Climate events over China? Part II: Extreme temperature. Front Environ Sci 10:921659. https://doi.org/10.3389/fenvs.2022.921659

Yao J, Chen Y (2015) Trend analysis of temperature and precipitation in the Syr Darya Basin in Central Asia. Theoret Appl Climatol 120:521–531. https://doi.org/10.1007/s00704-014-1187-y

Yao J, Zeng Y, Li J, Yang L (2020) A review of Dry-Wet Climate Change and Extreme Precipitation in Central Asia. Adv Meteorol Sci Technol 10:7–14. https://doi.org/10.3969/j.issn.2095-1973.2020.04.002

Yao J, Chen Y, Chen J, Zhao Y, Tuoliewubieke D, Li J et al (2021) Intensification of extreme precipitation in arid Central Asia. J Hydrol 598:125760. https://doi.org/10.1016/j.jhydrol.2020.125760

Zhang J, Wang F (2022) Future changes in extreme precipitation in Central Asia with 1.5–4°C global warming based on CMIP6 simulations. Int J Climatol 42(16):8509–8525. https://doi.org/10.1002/joc.7740

Zhang X, Alexander L, Hegerl GC, Jones P, Tank AK, Peterson TC et al (2011) Indices for monitoring changes in extremes based on daily temperature and precipitation data. Wiley Interdisciplinary Reviews: Clim Change 2(6):851–870. https://doi.org/10.1002/wcc.147

Zhang M, Chen Y, Shen Y, Li Y (2017) Changes of precipitation extremes in arid Central Asia. Quatern Int 436:16–27. https://doi.org/10.1016/j.quaint.2016.12.024

Zhang H, Li W, Li W (2019a) Influence of late springtime surface sensible heat flux anomalies over the tibetan and Iranian plateaus on the location of the south Asian high in early summer. Adv Atmos Sci 36:93–103. https://doi.org/10.1007/s00376-018-7296-2

Zhang M, Chen Y, Shen Y, Li B (2019b) Tracking climate change in Central Asia through temperature and precipitation extremes. J Geog Sci 29:3–28. https://doi.org/10.1007/s11442-019-1581-6

Zhang M, Yu H, Huang J, Wei Y, Liu X, Zhang T (2019c) Comparison of extreme temperature response to 0.5°C additional warming between dry and humid regions over East–central Asia. Int J Climatol 39(7):3348–3364. https://doi.org/10.1002/joc.6025

Zhang M, Yu H, King AD, Wei Y, Huang J, Ren Y (2020) Greater probability of extreme precipitation under 1.5°C and 2°C warming limits over East-Central Asia. Clim Change 162:603–619. https://doi.org/10.1007/s10584-020-02725-2

Zhang X, Hua L, Jiang D (2022) Assessment of CMIP6 model performance for temperature and precipitation in Xinjiang, China. Atmospheric Ocean Sci Lett 15(2):100128. https://doi.org/10.1016/j.aosl.2021.100128

Zhao P, He Z, Ma D, Wang W (2023) Evaluation of ERA5-Land reanalysis datasets for extreme temperatures in the Qilian Mountains of China. Front Ecol Evol 11:1135895. https://doi.org/10.3389/fevo.2023.1135895

Zhu X, Zhang M, Wang S, Qiang F, Zeng T, Ren Z et al (2015) Comparison of monthly precipitation derived from high-resolution gridded datasets in arid Xinjian, central Asia. Quatern Int 358:160–170. https://doi.org/10.1016/j.quaint.2014.12.027

Zhu X, Wei Z, Dong W, Ji Z, Wen X, Zheng Z et al (2020) Dynamical downscaling simulation and projection for mean and extreme temperature and precipitation over central Asia. Clim Dyn 54:3279–3306. https://doi.org/10.1007/s00382-020-05170-0

Ziegler K (2022) Implementation of improved land surface parameters and processes in the highly-resolved climate model REMO (Doctoral dissertation, Universität Würzburg). https://doi.org/10.25972/OPUS-26128

Zittis G, Hadjinicolaou P, Klangidou M et al (2019) A multi-model, multi-scenario, and multi-domain analysis of regional climate projections for the Mediterranean. Reg Enviqron Chang 19:2621–2635. https://doi.org/10.1007/s10113-019-01565-w